

AD-A102 346

BEDFORD RESEARCH ASSOCIATES MA
DEVELOPMENT OF MATHEMATICAL MODELS IN SUPPORT OF AFGL ATMOSPHER--ETC(U)
MAY 80 T M COSTELLO, J P NOONAN F19628-78-C-0083

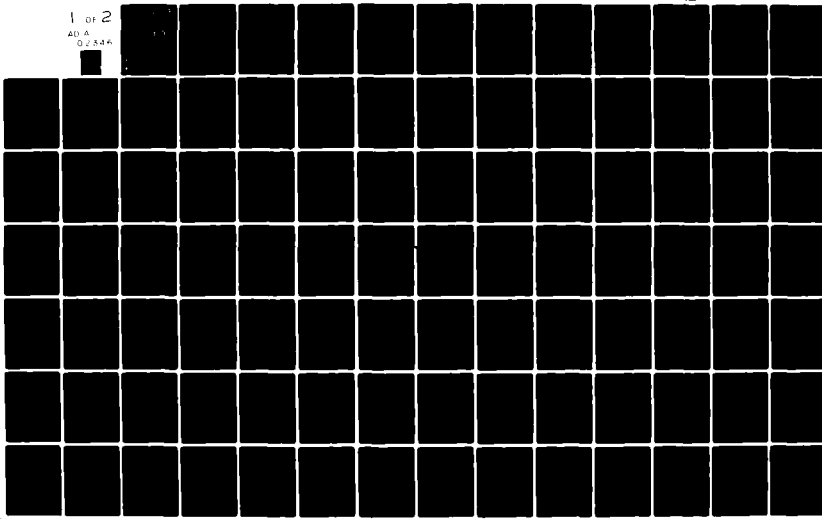
F/G 4/2

NL

UNCLASSIFIED

AFGL-TR-80-0296

1 of 2
AD A
02546



AD A102346

AFGL-TR-80-0296

LEVEL II

(12)
JW

DEVELOPMENT OF MATHEMATICAL MODELS IN
SUPPORT OF AFGL ATMOSPHERIC STUDIES

T.M. Costello
J.P. Noonan

Bedford Research Associates
2 DeAngelo Drive
Bedford, Massachusetts 01730

Final Report
April 1978 - April 1980

DTIC
ELECTED
AUG 03 1981
S E D
E

15 May 1980

Approved for public release; distribution unlimited

AIR FORCE GEOPHYSICS LABORATORY
AIR FORCE SYSTEMS COMMAND
UNITED STATES AIR FORCE
HANSOM AFB, MASSACHUSETTS 01731

DMC FILE COPY

817 31 070

**Qualified requestors may obtain additional copies from the
Defense Technical Information Center. All others should
apply to the National Technical Information Service.**

19 REPORT DOCUMENTATION PAGE		READ INSTRUCTIONS BEFORE COMPLETING FORM
1. REPORT NUMBER AFGL-TR-80-0296✓	2. GOVT ACCESSION NO. A D - A 202 346	3. RECIPIENT'S CATALOG NUMBER
4. TITLE (and Subtitle) Development of Mathematical Models in support of AFGL Atmospheric Studies.	5. TYPE OF REPORT & PERIOD COVERED FINAL REPORT April 1978 - April 1980	
7. AUTHOR(s) Thomas M. Costello Joseph P. Noonan	6. PERFORMING ORG. REPORT NUMBER FINAL REPORT	
9. PERFORMING ORGANIZATION NAME AND ADDRESS Bedford Research Associates 2 DeAngelo Drive Bedford, MA 01730	10. PROGRAM ELEMENT, PROJECT, TASK AREA & WORK UNIT NUMBERS 12) 11 11 16 9993XXXX 17 XX	
11. CONTROLLING OFFICE NAME AND ADDRESS Air Force Geophysics Laboratories Hanscom AFG, Mass. 01731 Monitor/Paul Tsipouras/SUWA	12. REPORT DATE 15 May 1980	
14. MONITORING AGENCY NAME & ADDRESS (if different from Controlling Office)	13. NUMBER OF PAGES	
	15. SECURITY CLASS (of this report) Unclassified	
	15a. DECLASSIFICATION/DOWNGRADING SCHEDULE	
16. DISTRIBUTION STATEMENT (of this Report) Approved for public release; distribution unlimited.		
17. DISTRIBUTION STATEMENT (of the abstract entered in Block 20, if different from Report)		
18. SUPPLEMENTARY NOTES		
19. KEY WORDS (Continue on reverse side if necessary and identify by block number) Deconvolution, IR Spectra, Magnetometer Network, Photoelectron Flux, Atmospheric Turbulence.		
20. ABSTRACT (Continue on reverse side if necessary and identify by block number) This report presents a summary of analyses and mathematical modelling done in support of some AFGL atmospheric research projects. In particular, work on the problems of loss of resolution due to instrument spreading, photo- electron flux modelling, atmospheric turbulence, and the magnetometer network are discussed.		

TABLE OF CONTENTS

	<u>Page</u>
Frequency Domain Interpretation of Iterative Deconvolution Techniques	5
An Estimate of the Effects of Temporal Background on System Performance	12
AFGL Magnetometer Network - A Program Overview	30
Magnetogram Processing	43
Some Properties of the Photoelectron Flux Equations	87
Angular Behavior of Photoproduction	109
Atmospheric Turbulence Modelling Impacting the Stratospheric Environment Program	114
Processing of Plasma Frequency Probe Data	123

Accession For	
NTIS GRA&I	<input checked="" type="checkbox"/>
DTIC TAB	<input type="checkbox"/>
Unannounced	<input type="checkbox"/>
Justification	
By	
Distribution/	
Availability Codes	
Dist	Avail and/or
	Special
A	

FREQUENCY DOMAIN INTERPRETATION OF
ITERATIVE DECONVOLUTION TECHNIQUES

INTRODUCTION:

Estimating the input to a linear systems when the output (corrupted by noise) and the system function are known, is called the deconvolution problem. Many approaches to the solution of the problem involve iterative time domain techniques. Here, we provide a frequency domain interpretation of these techniques.

Formulation of the Problem

The problem may be viewed mathematically as follows:

Define:

Input	$I(t)$
Output	$O(t)$
Instrument function	$h(t)$
Measured noise	$n(t)$

Since the instrument is a linear system, $I(t)$ and $O(t)$ are related by the convolution integral (* denotes convolution).

$$O(t) = I(t) * h(t) + n(t)$$

or

$$O(t) = \int I(\tau) h(t-\tau) d\tau + n(t)$$

In the problem we are addressing, $O(t)$ and $h(t)$ are known (measured and we wish to estimate $I(t)$).

Solution Methods

The reference papers provide a summary of some of the approaches that have been employed to solve this problem.

Most of those techniques employ iterative methods.

Historically the noise term has been (formally) ignored and the deconvolution has been viewed as a Fredholm integral equation of the first kind. The iterative techniques which have been employed use the concept of successive substitutions. (1,2)

- The basic types of algorithm in these iterative methods are a variation of the following: with $O(t)$ the measured output,

$$\begin{aligned} I_1(t) &= O(t) + [O(t) - O(t) * h(t)] \\ &\vdots \\ I_n(t) &= I_{n-1}(t) + [O(t) - I_{n-1}(t) * h(t)], \end{aligned}$$

finally

$$\hat{I}(t) = I_n(t) \text{ for some predetermined } n$$

(\hat{I} , denotes the estimated input)

Minimum Mean Squared Error Solution (MMSE)

Viewing this problem as similar to the system identification problem where $h(t)$ is unknown [12, 13], consider deriving the MMSE estimate for $I(t)$. The MMSE estimate would have the interpretation of having the smallest variance of any possible estimate of $I(t)$.

Thus from Eq. (1) we wish to choose $I(t)$ to minimize the expected value (statistically) of ϵ^2 where:

$$\epsilon = E \{ N(t) \} = E \{ O(t) - \int I(\tau) h(t-\tau) d\tau \}$$

That is find $I(t)$ such that

$$\text{Min } \epsilon^2 = \text{Min } E \{ N(t)^2 \}$$

$$(2) \quad = \text{Min } E \{ \{ O(t) - \int I(\tau) h(t-\tau) d\tau \}^2 \}$$

where

E denotes the mathematical expectation (statistical average). Under the assumption that $N(t)$ is not correlated with $h(t)$, it is well known (as a consequence of the orthogonality principle) that the solution to Eq. (2) leads to the Wiener-Hopf equation,

$$(3) \quad \Theta_{oh}(t) = \int I(\tau) \Theta_h^2(t-\tau) d\tau$$

where

Θ_h^2 is the autocorrelation of the system function $h(t)$

and Θ_{oh} is the cross correlation of the output and system functions, $O(t)$ and $h(t)$ respectively.

This equation may be solved for $I(t)$ using Fourier transform techniques.

Letting

$$\begin{aligned} F \left\{ \Theta_{oh}(t) \right\} &\equiv \Phi_{oh}(\omega) \\ F \left\{ \Theta_h^2(t) \right\} &\equiv \Phi_h^2(\omega) \end{aligned}$$

and

$$F \left\{ I(t) \right\} \equiv I_f(\omega),$$

we obtain

$$(4) \quad I_F(\omega) = \frac{\Phi_{oh}(\omega)}{\Phi_h^2(\omega)}$$

(assuming $\Phi_h^2(\omega)$ is not zero over the range of ω considered)

Finally taking the inverse Fourier transform

$$(5) \quad \hat{I}(t) = F^{-1} \left[\frac{\Phi_{oh}(\omega)}{\Phi_h^2(\omega)} \right]$$

Note that the FFT may be employed to perform the required calculations.

If there is no noise i.e. $N(t) = 0$, (5) will yield the exact solutions to (1).

When noise is present some smoothing of the spectral estimate $\Phi_{oh}(\omega)$ will be required to produce a stable estimate.

There is a basic trade-off between increased resolution of peaks in $I(t)$ and noise performance. That is, in the presence of noise, erroneous noise spikes appear in $I(t)$ as increased resolution is demanded. In fact, with no spectral smoothing [highest resolution possible] virtually no noise can be tolerated. This is due basically to the fact that, without smoothing, the MMSE criterion minimizes the square error integrated over the signal space. Hence, MMSE is somewhat insensitive to noise spikes.

Iterative Method as a Special Case of the MMSE Approach

Following the presentations of [2] and [8], one can show that the iterative solution (after n iterations) can be expressed as follows:

$$\begin{aligned} I_n(t) &= (n+1)O(t) - \binom{n+1}{2} h(t) * O(t) \\ &+ \binom{n+1}{3} h(t) * h(t) * O(t) \\ &+ \dots + h(t) * \dots * h(t) * O(t) \\ &\quad n \text{ times} \end{aligned}$$

Taking the Fourier transform of both sides and collecting terms we have

$$\begin{aligned} I_F(\omega) &= O_F(\omega) \cdot (n+1) \\ &+ \sum_{m=1}^n (-1)^m \binom{n+1}{m+1} H_F^m(\omega) O_\phi(\omega) \\ &= \sum_{m=0}^n (-1)^m \binom{n+1}{m+1} H_F^m(\omega) O_\phi(\omega) \\ &= \frac{H_F^*(\omega) \cdot O_F(\omega)}{|H_F(\omega)|/2} \cdot \underbrace{\sum_{m=0}^n (-1)^m \binom{n+1}{m+1} H_F^{m+1}(\omega)}_{\text{Smoothing Function}} \end{aligned}$$

Unsmoothed MMSE

Smoothing Function

Using

$$\frac{H_F^*(\omega) \cdot O_F(\omega)}{|H_F(\omega)|^2} = \left[\frac{\Phi_{oh}(\omega)}{\Phi_h^2(\omega)} \right]$$

in combination with (4), (5) and this, last equation shows that the iterative method may be viewed as the MMSE method with the spectral smoothing function given by:

$$S(\omega) = \sum_{m=0}^n (-1)^m \binom{n+1}{m+1} H_F^{m+1}(\omega)$$

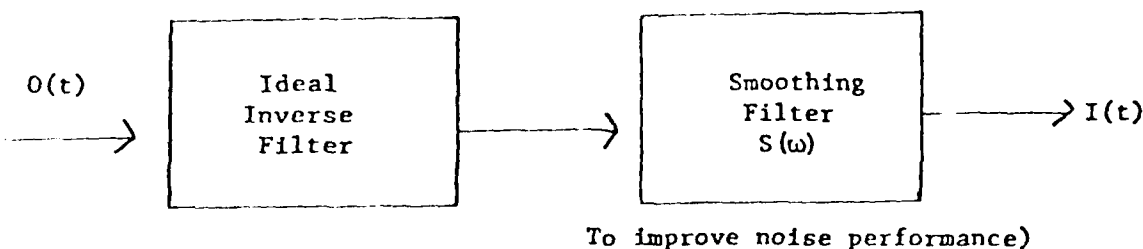
or

$$\sum_{m=1}^{n+1} (-1)^{m-1} \binom{n+1}{m} H_F^m(\omega)$$

This is depicted in Figure 1 below.

Parallelling the derivations [12] and [13] one can establish (assuming Gaussian noise $N(t)$) that

$\hat{I}_F(\omega)$ is an F distributed random variable where the degrees of freedom depend on the smoothing function $S(\omega)$.



Frequency Domain Interpretation of Iterative Deconvolution Techniques.

FIGURE 1

R E F E R E N C E S

1. "Iterative unfolding of intensity data, with application to molecular beam scattering.", Siska, P.E., The Journal of Chemical Physics, Vol. 59, 11, December 1973, pp. 6052-59.
2. "Smoothing and Unfolding the Data of Beam-Collision Experiments", Ioup, G.E. and B.S. Thomas, The Journal of Chemical Physics, Vol. 46, 10, May 1967, pp. 3959-61.
3. "On the Optimum Use of Ionization-Efficiency Data", Morrison, J.D., The Journal of Chemical Physics, Vol. 39, 1, July 1963, pp. 200-07.
4. "Minimum-Bias Windows for High Resolution Spectral Estimates", Papoulis, A., IEEE Transactions on Information Theory, Vol. IT-19, 1, January 1973, pp. 9-12.
5. "On Deconvolution Using the Discrete Fourier Transform", Silverman, Harvey and Allan E. Pearson, IEEE Transaction Audio Electroacoust., Vol. AU-21, April 1973, pp. 112-118.
6. "A Technique for the Numerical Solution of Certain Integral Equations of the First Kind", Phillips, D.L., Argonne National Laboratory, pp. 84-97.
7. "A Theorem on the Difficulty of Numerical Deconvolution", Abstract, IEEE Transactions on Audio and Electroacoustics, March 1972.
8. "Aerial Smoothing in Radio Astronomy", Bracewell, R.N. and J.A. Roberts, Australian J. Phys., 7, 1954.
9. "A Technique for the Numerical Solution of Certain Integral Equations of the First Kind", Phillips, David L., Journal of the Association for Computing Machinery Vol. 9, 1962, pp. 84-87.
10. "On the Numerical Solution of Fredholm Integral Equations of the First Kind by the Inversion of the Linear System Produced by Quadrature", S. Twomey, Journal of the Association for Computing Machinery, Vol. 10 1963, pp. 97-101.
11. "The Application of Numerical Filtering to the Solution of Integral Equations Encountered in Indirect Sensing Measurements", Twomey, S., Journal of the Franklin Institute, Vol. 270, 2, January 1965, pp. 95-109
12. "Spectral Analysis and Its Applications", G.M. Jenkins and D.G. Watts, Holden-Day, 1968, Chapter 10.
13. "Random Data: Analysis and Measurement Procedures", J.S. Bendat and A.G. Piersol, John Wiley and Sons, Inc. 1971, Chapter 6.

AN ESTIMATE OF THE EFFECTS OF TEMPORAL
BACKGROUND ON SYSTEM PERFORMANCE

1. INTRODUCTION

In order to evaluate the performance of an infrared sensor, the system designer needs to know the spatial and temporal characteristics of the background. With these data and a knowledge of platform instabilities he can systematically design a sensor and predict its sensitivity, false alarm rate and detection probability. When one considers a mosaic staring sensor, spatial and temporal variations in the background affect the performance in two ways. First, platform instabilities can cause radiance variations from the spatially structured terrain and second time variant changes in the background will cause a response in the sensor.

Over the past several years, techniques for the performance analysis of advanced surveillance systems have been developed. Much of the work has been limited however to analysis of spatial variations in the background obtained from various measurement programs. Among these are:

- RM-19 Satellite Experiment (Lockheed) - The RM-19 experiment was designed to obtain background measurements from a low altitude, high-inclination, circular orbit, in a number of spectral bands near 2, 4 and 6 μm . Spectral, spatial and exceedance data were obtained and represent one of the major sources of background data from space.
- BMP - CAMP Experiment (Lockheed U-2) - The Lockheed U-2 program was designed to measure spatial characteristics of various background sources in the blue and red spike region of 4 μm as well as at various wavelengths in the LWIR region 14 μm .

Valuable PSD data have been made available through this program, which shows the dependence on terrain and cloud types as well as the variation of PSD from MWIR to LWIR.

- KC-135 flights (AFGL) - High resolution spectra: $\Delta\sigma = 4 \text{ cm}^{-1}$ and $\Delta\sigma = 1 \text{ cm}^{-1}$ of several classes of terrain and cloud backgrounds have been measured from KC-135 aircraft. These data have been used to establish bench marks to calibrate the emission and reflection models from terrain and clouds as a function of solar zenith and azimuth angles.
- U-2 flights (A.D. Little) - Additional cloud spectral data are available from the A.D. Little U-2 flights. These consist of a series of observations of clouds of varying types, and over a range of viewing conditions in the $2 \mu\text{m}$ region. These data are useful to provide a range of variation to be expected in cloud spectra.
- ERIM flights - High spatial resolution data was obtained over desert and mountainous terrain, over rural and urban terrain and over water. Spatial resolution was two to three feet. Data was collected in six selected bands from 2 to $5.7 \mu\text{m}$ as well as the spectral band from 2 to $11.4 \mu\text{m}$. The primary interest in these data is its two dimensional nature. Unfortunately, two dimensional data are not presented, the presentation being in-track and cross-track power spectra.

All of these programs were concerned with spectral and spatial variations of terrain and cloud backgrounds. Although there has been work on modelling temporal backgrounds,¹ temporal background data has not been available. It is expected that a strong source of temporal fluctuations would be moving clouds. In the absence of experimental data, a random process model was postulated to obtain power spectral density estimates. It is the purpose of this paper to present this model and to estimate the effect of this clutter on system performance.

2. LWIR CLOUD TEMPORAL CLUTTER MODEL

Consider a broken cloud distribution moving past a starting sensor. If we assume the cloud is opaque, the radiance observed at the sensor represents the radiation from a blackbody at the temperature of the ambient air at the cloud altitude. When the atmosphere is clear, the sensor would observe the warm terrain. To illustrate this situation a hypothetical trace is shown in Figure 1. This illustrates the radiance fluctuations that a downward looking sensor would observe generally at a wavelength of 9 μm for clouds at 3 or 6 km. It is reasonable to assume that the random arrival of clouds may be modelled as a Poisson process² with arrival parameter adjusted for an assumed percentage of cloud cover. For the calculations that follow a 50% cloud cover is assumed. A typical sample of Poisson arrivals is shown in Figure 2. The effect of a cloud on the measured radiance depends on the wavelength and the altitude, speed, size and shape of a cloud passing through the field of view. For the purpose of this paper, we have assumed a sensor operating at 9 μm viewing terrain with broken clouds at 6 km altitude. The idea is to allow clouds to enter the field-of-view, reach a maximum image of radiance and then exit. The effect of a cloud on the radiance trace was assumed to take one of the forms shown in figure 3. Obviously, many shapes may be assumed but it is felt that those shown would be representative of the problem allowing for an upper limit of fast entry and exit as well as for a smooth entry and exit, thus bounding the probable spectral roll-off that could occur with an actual cloud.

The time required for entry and exit and the duration of time the cloud is in the field-of-view depends on the size and speed of a cloud. The radiance waveform (figure 3) may be coupled with the Poisson arrival process by convolving the shape with the Poisson impulses. This yields what is commonly called a "shot noise" process model.

If we denote the cloud shape trace (Figure 4) by $h(t)$, the assumed process may be represented as²

$$h(t) = \sum_{i=-\infty}^{\infty} h(t - t_i) \quad (1)$$

where t_i are Poisson random time arrivals. The statistical autocovariance function for the process $g(t)$ is obtained by convolving the process with itself.² Thus:

$$C(T) = \lambda \int_{-\infty}^{\infty} h(\alpha)h(T + \alpha) d\alpha \quad (2)$$

The power spectrum, the fourier transform of $C(T)$ can be obtained from the impulse response $h(t)$ and is given by

$$S(\omega) = \lambda |H(\omega)|^2 \quad (3)$$

The fourier transform of $h(t)$ is given as

$$H(\omega) = F[h(t)] \quad (4)$$

For the waveforms of Figure 3, the corresponding $H(\omega)$ are as follows:

$$(a) H(\omega) = A T_0 \frac{\sin \omega T_0/2}{\omega T_0/2} \quad (5) \text{ reference 3}$$

$$(b) H(\omega) = \frac{2A}{b-a} \frac{\cos a \omega - \cos b \omega}{\omega^2} \quad (6) \text{ reference 3}$$

$$(c) H(\omega) = A \frac{T_0}{2} (1 - 2\alpha) \frac{\sin \omega T_0/2 (1-2\alpha)}{\omega T_0/2 (1-2\alpha)} \\ + \frac{T_0}{2} \frac{\sin \omega T_0/2}{\omega T_0/2} - \cos \alpha \omega T_0/2$$

$$\cdot \sin \omega T_0/2 (1 - \alpha) \frac{\omega^2}{\omega^2 - \frac{4\pi^2}{4\alpha^2 T_0^2}} \quad (7) \text{ reference 4}$$

3. CALCULATED RESULTS

For the results that follow, footprints of 200 m and 1 km were chosen as a representative. For the 200 m footprint we arbitrarily assumed cloud sizes of 200 m, 500 m, 1 km and 5 km. For the 1 km footprint we assumed cloud sizes of 1 km, 5 km and 10 km. We assumed cloud speeds of 10 and 30 m/sec which are not unreasonable speeds based on data shown in Figure 4.⁵ As indicated earlier, a 50% cloud cover was assumed. Cloud size and velocity were separately evaluated so that 14 separate cases were treated for both the simple trapezoidal waveform Equation (6) and cosine trapezoid Equation (7). The power spectrum for each case was calculated. Selected PSD are presented in the following figures to show the effects of cloud size, speed and type of waveform. All clouds are assumed to be at 6 km altitude. For clouds at 3 km the results should be divided by 2. Figure 5 shows the PSD* of the random arrival of 200 m clouds moving at a speed of 10 m/sec assuming a cosine trapezoidal waveform. The first null occurs at approximately 0.05 Hz with a roll off of approximately $f^{-5.5}$. The same situation is shown in Figure 6 except for a trapezoidal waveform. The first null occurs at approximately the same frequency. However, the roll off is now changed to $f^{-3.5}$. The effect of the increase in velocity is shown in Figure 7 for the same conditions shown in Figure 5. The velocity of the clouds are now 30 m/sec. The first null has shifted to a higher frequency approximately 0.15 Hz and the roll off is now f^{-4} .

The situation for larger footprint is shown in the next two figures. Figure 8 shows the PSD of 1 km clouds moving at speeds of 10 m/sec across a 1 km footprint. The first null now occurs at 0.01 Hz with a roll off of approximately f^{-0} . Figure 9 shows the PSD of 10 km clouds moving at speeds of 30 m/sec across a 1 km footprint. The first null occurs at a frequency of approximately 0.002 Hz with a roll off of f^{-5} .

⁵Valley, S.L., Editor, Handbook of Geophysics and Space Environments, 1965
*The PSDs should read log PSD in the figures.

The rectangular waveform of Figure 3 (a) is not considered realistic since clouds will not enter or exit that abruptly. However, this waveform serves as an upper bound on the high frequency roll off rate f^{-2} . The first null of the spectra depends on the duration of the pulses γ_2/T . This is consistent with the results shown in Figures 5 through 9. Thus, the speed and size of the cloud dictate the bandwidth of the spectra.

The RMS clutter leakage was obtained for each case by filtering through first, second, and third differencing algorithms. For 200 m footprints, a frame time of 1 sec was used. For km footprint, a frame time of 5 sec was used. Results for third differencing are plotted in Figure 10. In the figure, the clutter leakage is shown vs. cloud size with cloud speed and footprint as parameters. For all the cases considered, the clutter leakage varies over the range from $10\text{-}100 \text{ kw/cm}^2 \text{ sr } \mu\text{m}$.

For a more realistic situation one can combine a number of different cloud sizes moving at a constant speed at a given altitude or combine clouds at different altitudes with different speeds. Assuming they are independent the spectra would add since the cross covariances are zero. This results in a spectra model given by

$$S(\omega) = \sum_{j=1}^N p_j \lambda_j H_j(\omega)^2 \quad (8)$$

where

p_j = probability of a j cloud type

λ_j = arrival rate of cloud type j

$H_j(\omega) = F[h_j(t)]$

Figure 11 shows the PSD of the combination of cloud sizes from 200 m to 5 km moving at a constant velocity of 10 m/sec across a 200 m pixel. The resulting spectra as expected is intermediate between those shown in Figures 5 - 9.

4. CONCLUSIONS

The results of these calculations show that moving clouds under the conditions described in this paper represent a rather severe clutter problem for LWIR downward systems. For system footprints on the order of 200 m the clutter noise would vary over the range 4 kw/sr μm to 40 kw/sr μm .

The work performed above represents a first order approximation to cloud clutter at LWIR wavelengths. For a more refined model one must consider realistic cloud situations. Instead of taking an average of cloud sizes as above, one should more properly expect the occurrence of (at least for cumulus clouds) larger clouds to decrease exponentially.⁶ Still another modification is needed to correct for the spatial transfer function of the sensor. This would, of course, have more of an effect on smaller sizes.

⁶Palink, V.G., The Size Distribution of Cumulus Clouds in Representative Florida Populations, J. Appl. Meteorology, Vol. 8, 1969.

R E F E R E N C E S

1. Lee, M., Mosaic Sensor Study (U), Aerospace Report No. 243, 1975.
SECRET
2. Papoulis, A., Probability, Random Variable, and Stochastic Processes, McGraw-Hill, 1965.
3. Lathi, B.P., Signals, Systems and Communications, John Wiley & Sons, 1965.
4. Childers, D. and Durking, A., Digital Filtering and Signal Processing, West Publishing Co., 1975.

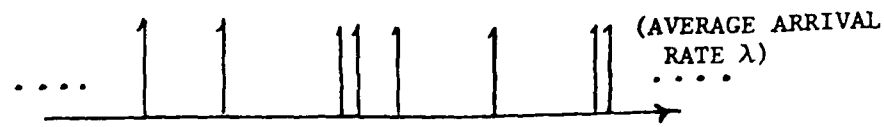


$$A = 400 \frac{\mu W}{cm^2 sr \mu m} \text{ FOR CLOUD AT } 6 \text{ km}$$

$$A = 200 \frac{\mu W}{cm^2 sr \mu m} \text{ FOR CLOUD AT } 3 \text{ km}$$

FIGURE 1

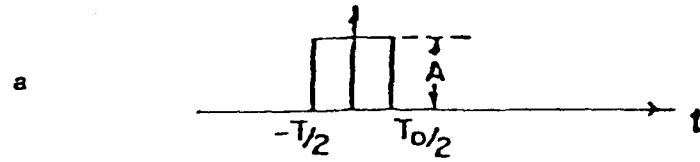
Hypothetical radiance trace observed
by a down looking sensor for a standard
atmosphere with clouds at altitude of 3 and 6 km.



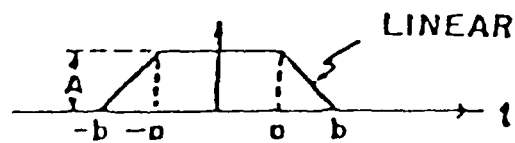
"TYPICAL" POISSON ARRIVAL PROCESS

FIGURE 2

A typical sample of Poisson Arrival.



b



c

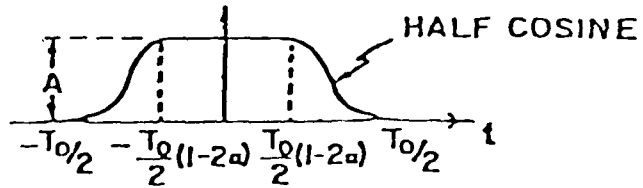


FIGURE 3
Assumed radiance trace waveforms
for the Paper

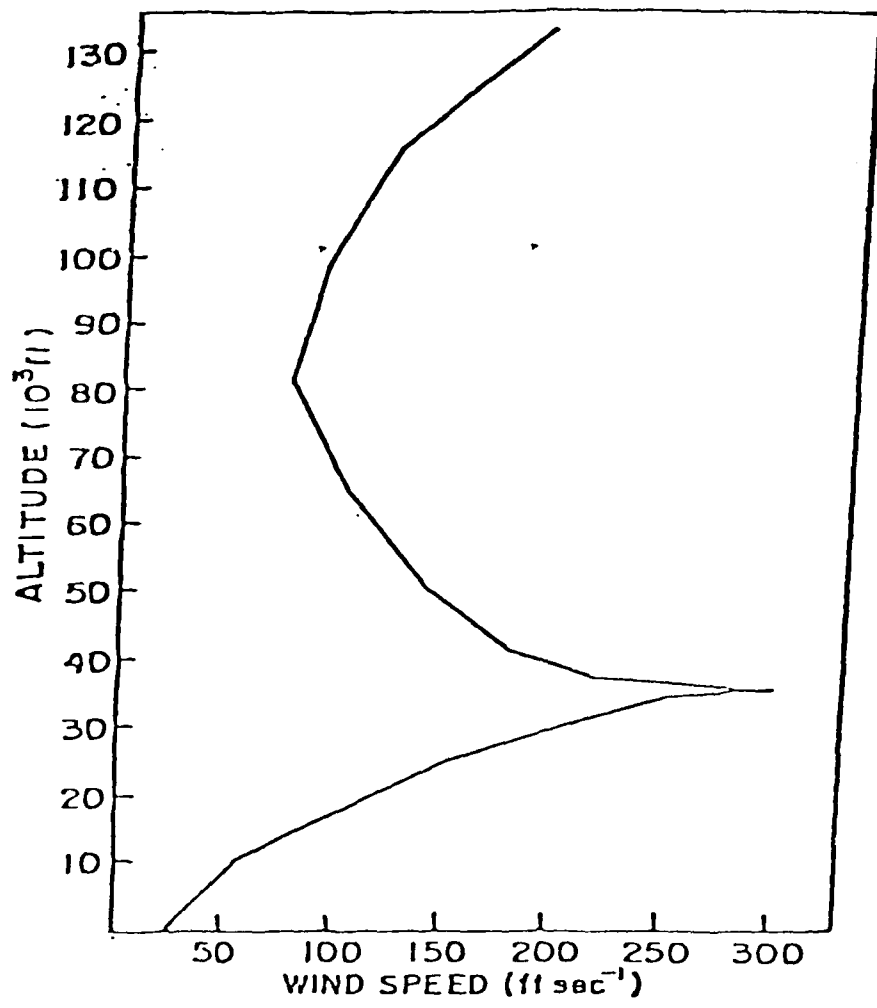


FIGURE 4

Maximum wind speeds likely to be exceeded only
1% of wintertime over northeastern USA.

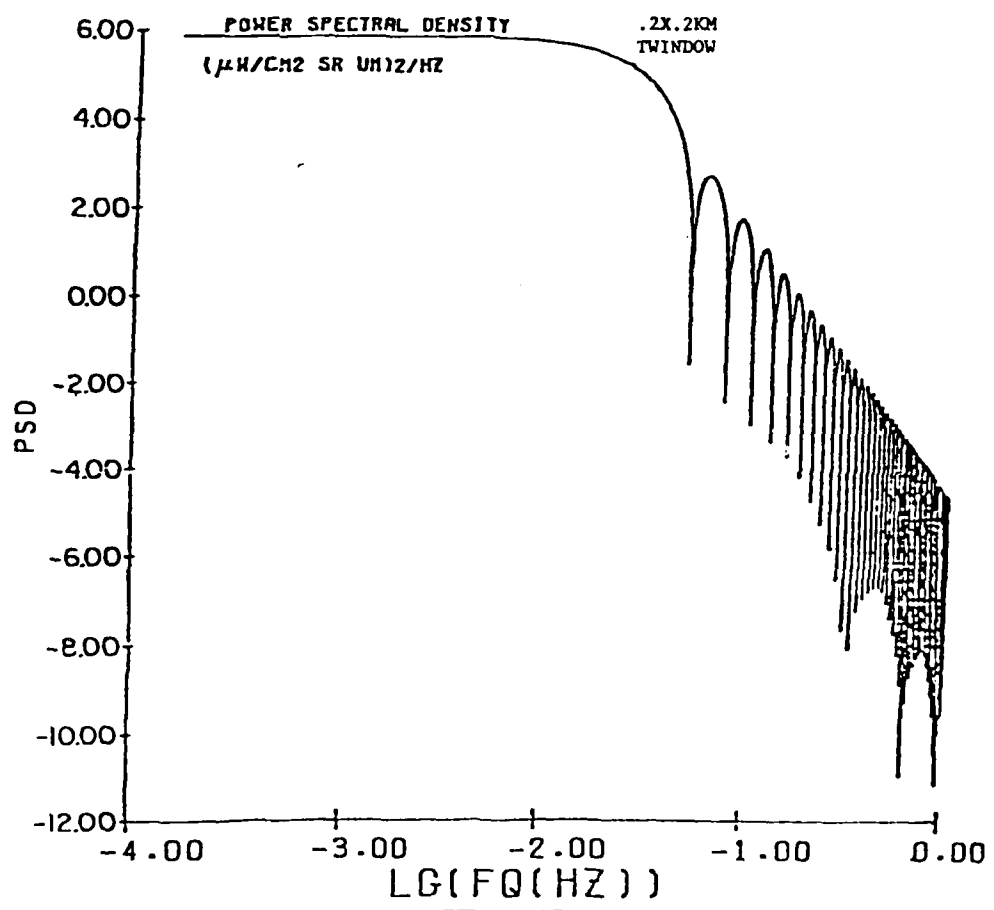


FIGURE 5

The PSD of 200M clouds moving at a speed of
 10 m/sec across a 200 m pixel using waveform
 Fig. 3C.

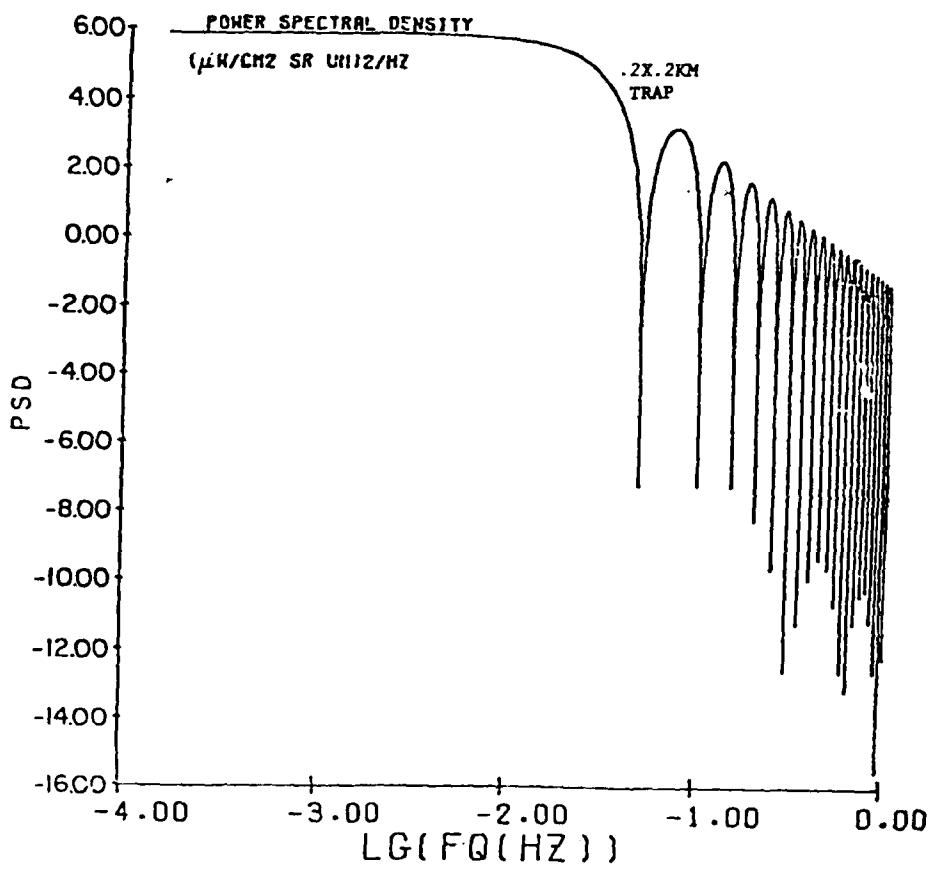


FIGURE 6

The PSD of 200m clouds moving at a speed of
10 m/sec across a 200 m pixel using waveform
Fig. 3B.

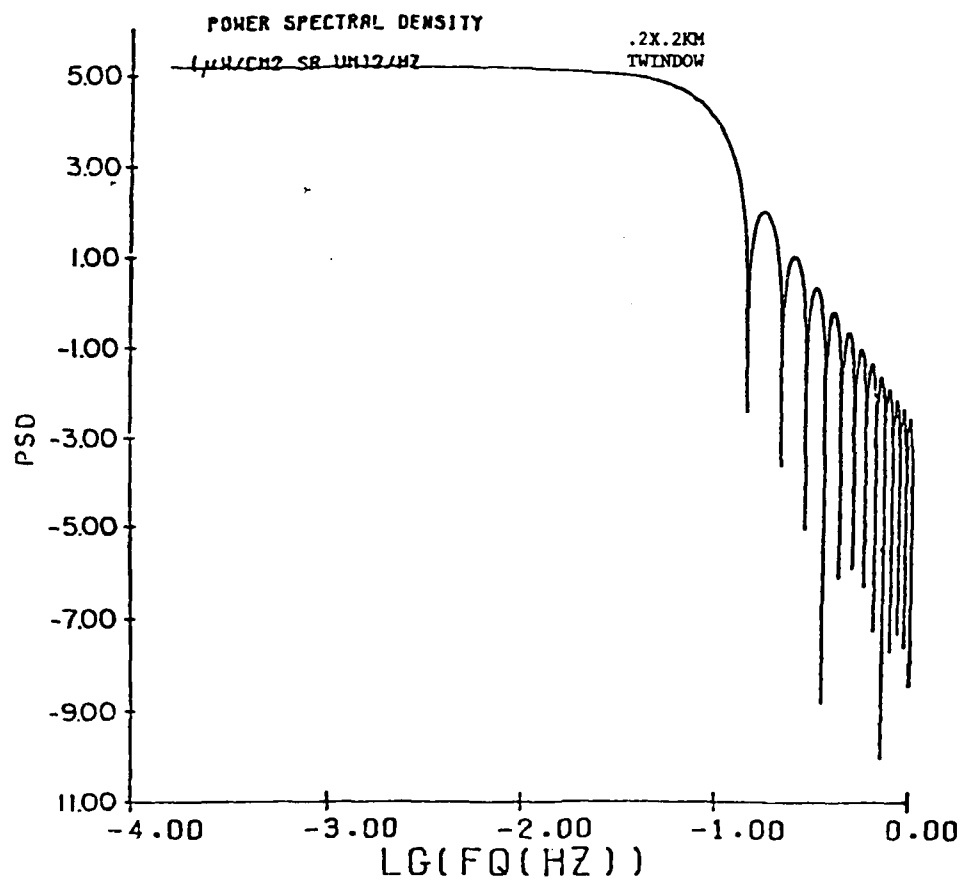


FIGURE 7

The PSD of 200 m clouds moving at 30 m/sec across a 200 m pixel using waveform Fig. 3C.

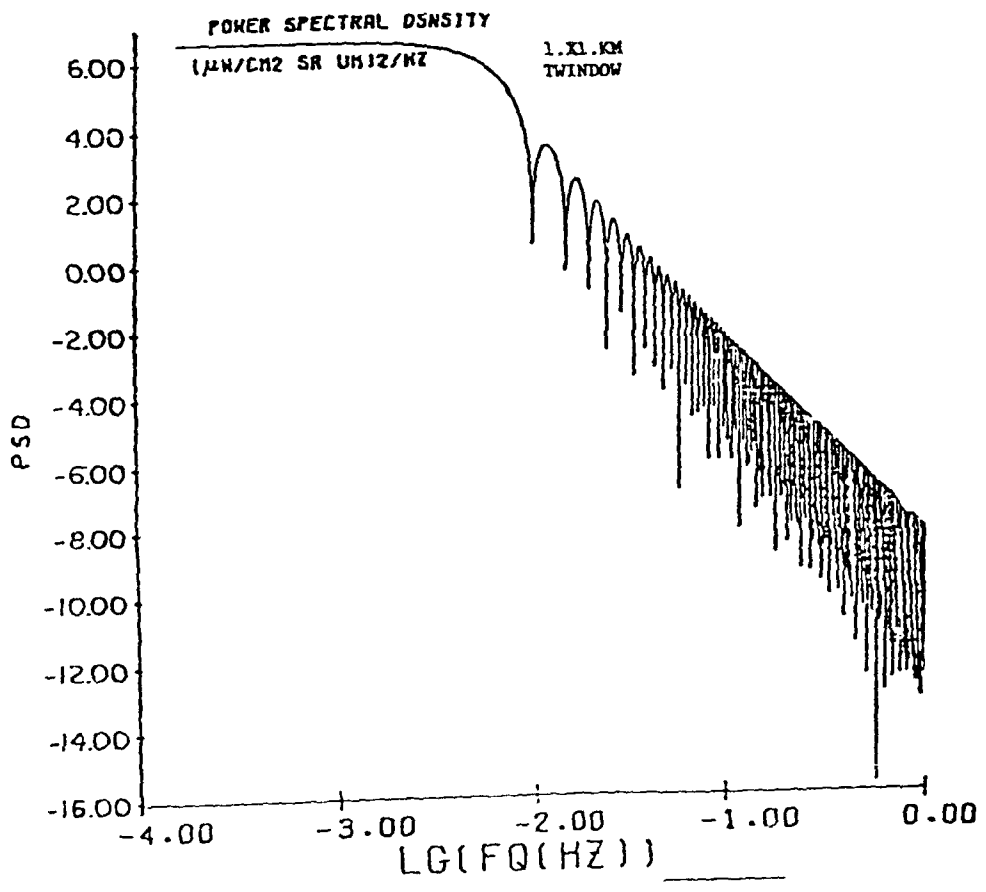


FIGURE 8
The PSD of 1 km clouds moving at 10 m/sec
across a 1 km pixel using waveform Fig. 3C.

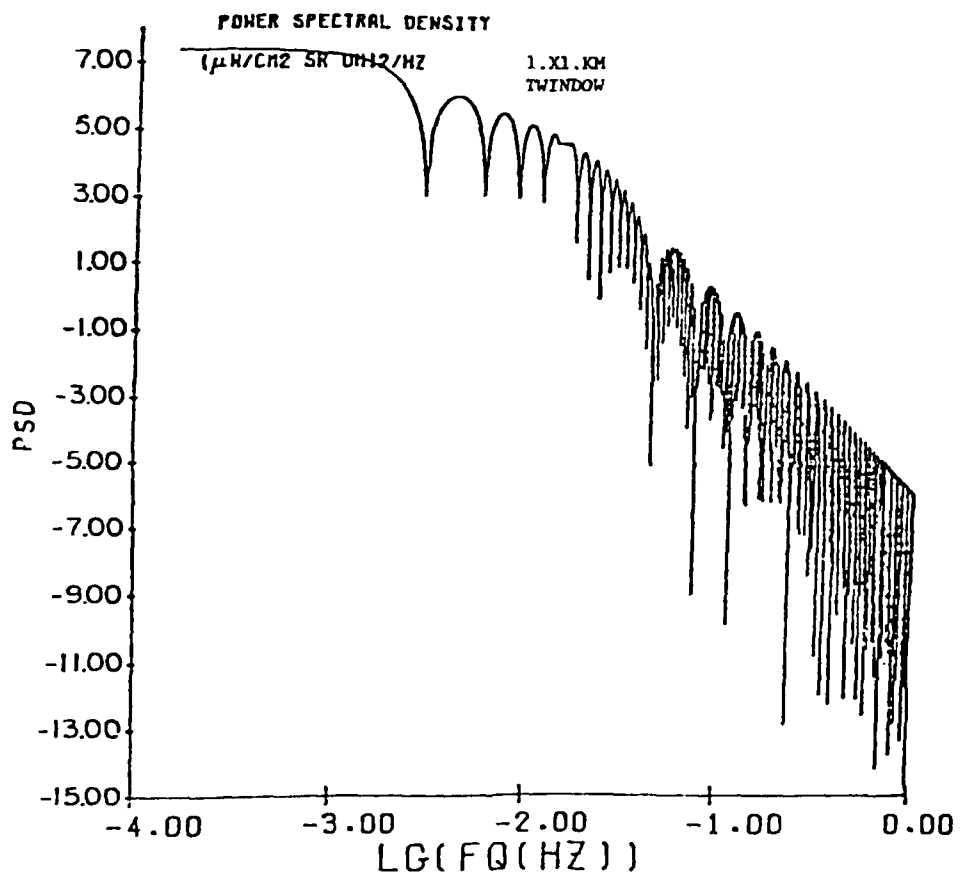


FIGURE 9

The PSD of 10 km clouds moving at 30 m/sec across a 1 km pixel using waveform Fig. 3C.

CLUTTER LEAKAGE THIRD DIFFERENCING

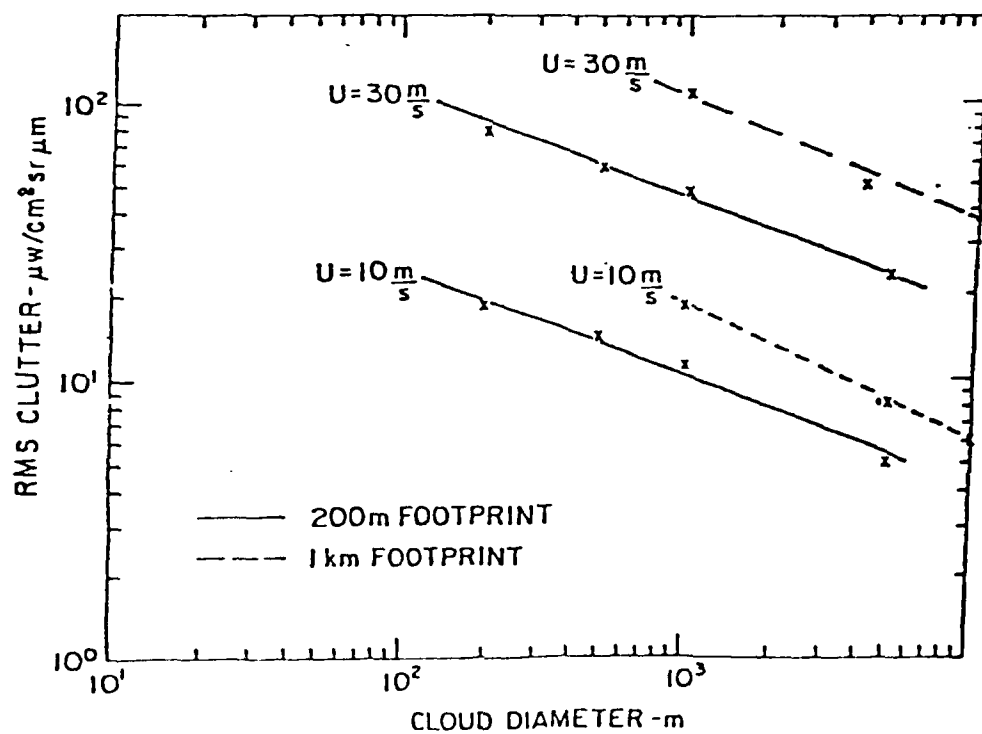


FIGURE 10

Clutter Leakage vs. Cloud size

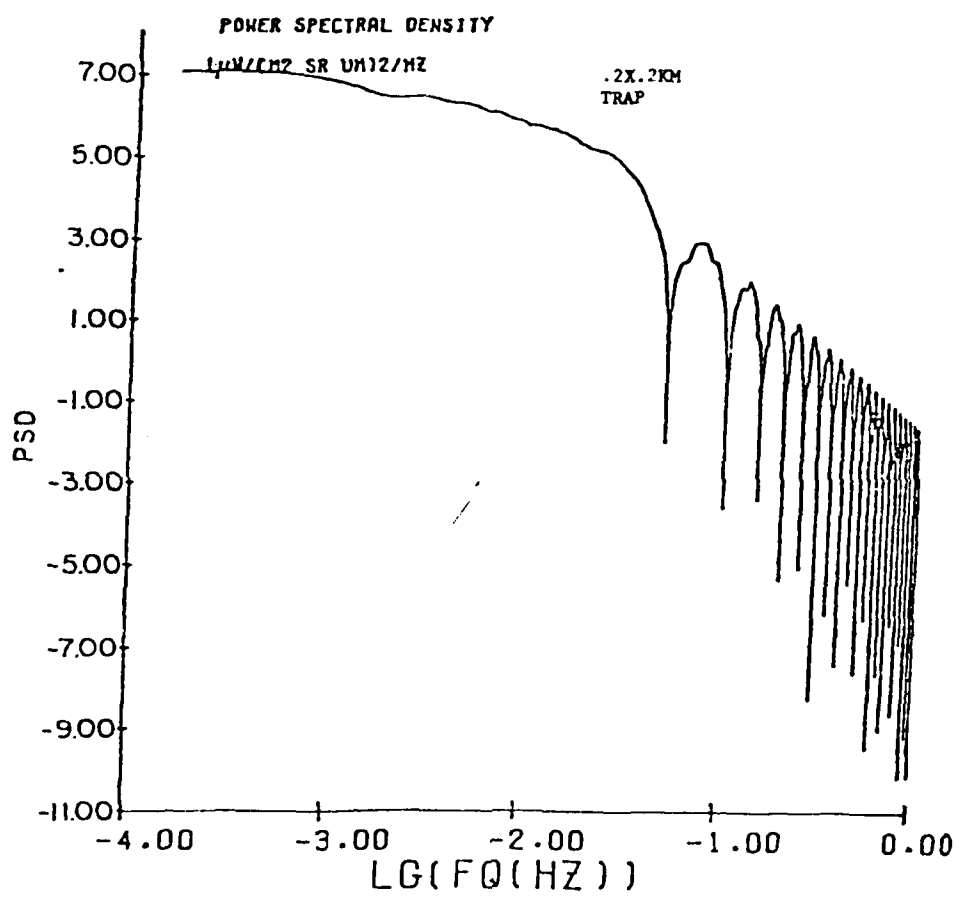


FIGURE 11

The PSD of combining cloud sizes from 200 m to 5 km moving at 10 m/sec across a 200 m pixel using waveform Fig. 3B.

AFGL MAGNETOMETER NETWORK

A Program Overview

The goal of this task is to use the AFGL Magnetometer Network data base to improve the Air Force's ability to specify and predict geomagnetic activity. This information is very useful in the studying of propagation of electro-magnetic waves and messages in the atmosphere. Initial efforts are aimed at generating an easily accessible data base for 1-2 years of data. Subsequent work will use the data in spectral and maximum entropy modelling.

Projected users of this data and analysis include Headquarters of Air Weather Service, AFSATCOM, and SAC.

INTRODUCTION

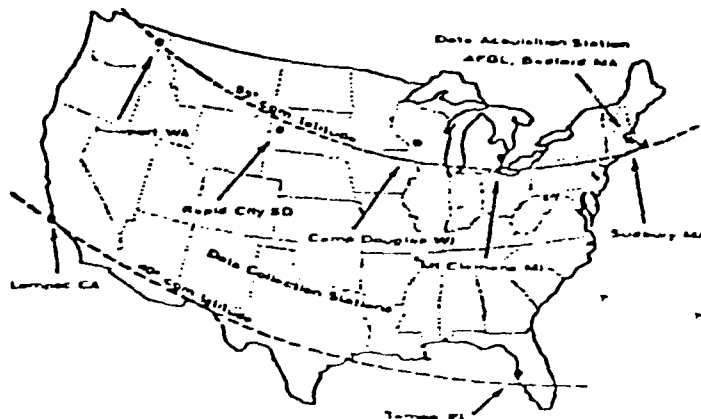
Space affects operational systems because it is a dynamic environment with daily and seasonal variations and with naturally occurring disturbances. A complete understanding of naturally occurring disturbances in the magnetosphere and the ionosphere requires an understanding of the solar contribution to such disturbances. The Air Force is concerned with the degrading effects on its communications and surveillance systems which result from interaction of those systems with a dynamic space environment. However, the occurrence of the magnetic storms or proton showers which cause these disturbances cannot be predicted without a knowledge of the solar activity which causes them.

During periods of high solar activity, a greatly enhanced charged particle population propagates from the sun through interplanetary medium. The solar energetic particles emitted from the sun on interplanetary magnetic field lines leading from the sun to the vicinity of the earth will travel through the earth's magnetosphere and impinge on the polar ionosphere. Solar particle events have a deleterious effect not only on polar communication systems but also on satellite sensors that are irradiated by solar particle fluxes.

AEROSPACE MAGNETIC MONITORING

The ability to specify magnetic activity levels in real time and to predict such activity hours in advance is urgently needed to support various Air Force agencies, including AFSATCOM, SAC, NORAD AND AFGWC. Other users would include SAMSO, ARPA and the various groups engaged in fuel and mineral surveys. A program for specification and prediction requires a system for

the collection of magnetic activity data, its transmission to a central station and the means for near real-time operation on the data. This is being done by the AFGL magnetic monitoring network.



Geographical locations of the stations in the AFGL Magnetometer Network.

Severe magnetospheric disturbances, called magnetosphere storms, produce a variety of adverse effects on operational military systems. The effects result from severe departures from the normal ionospheric and magnetospheric conditions upon which systems such as military communications depend for operation. The objectives of the AFGL Magnetometer Network program include the development of methods to predict magnetospheric storms in order to lessen their impact on military operational capability and the provision of real time data to operational military systems which require a knowledge of magnetospheric conditions for optimum performance.

A magnetospheric storm produces a number of phenomena; its manifestation as a disturbance of the geomagnetic field is called a magnetic storm. The AFGL program chooses the magnetic field as the parameter to be studied because of its direct dependence on the basic processes producing the disturbance and the relative ease with which it may be measured by ground

magnetometers. The practical approach chosen is to measure magnetic-field disturbances at a number of selected locations in the United States with magnetometers which cover an appropriate range of amplitude and frequency and to transmit the resulting data in real time to a central location. The data obtained are measurements of the vector magnetic field at intervals of one second and measurements of the vector time derivative of the field for fluctuations with periods between one and 1000 seconds.

Each instrumented data-collection station (DCS) operates continuously and automatically, unattended except for routine maintenance. Five stations are located approximately along the line of 55°N corrected geomagnetic latitude, and two additional stations lie along the line of 40°N corrected geomagnetic latitude. Data from each station are returned in real time on commercial voice-grade communication circuits to a single data-acquisition station (DAS) located at the Air Force Geophysics Laboratory at Hanscom Air Force Base, Massachusetts. The DAS performs real time processing, reduction, and display of the data and stores processed data in a permanent file for subsequent analysis. All facilities involved are dedicated to the program, so essentially uninterrupted operation over an extended time period is possible.

The important features of the magnetometer network are (a) the ordered array of stations, (b) the measurement of both the vector field and its time derivative at a rapid sampling rate by identical instruments producing directly comparable data, (c) the transmission of these data in real time to AFGL, (d) the automatic real time processing.

All data words are 11 bits in length, with four parity bits added for error-correction purposes. Thus, a frame of data, as prepared for transmission, consists of 240 15-bit words; these are stored in a matrix constructed of 15 240-bit shift registers. Since one sampling interval

follows the preceding one without pause, while data from each interval need to be stored until the assigned transmission time (between zero and ten seconds later), two identical matrices are used in alternation, each being filled in one ten-second interval and storing/transmitting in the next. The output is a serial stream of 3600 bits (240 words of 15 bits each) clocked out at a rate of 4800 bits/sec; the duration of the bit stream is therefore 750 ms.

In addition to the redundant coding obtained by using four parity bits, a technique of interleaving bits from all the words is used to reduce the effect of a noise burst lasting longer than the duration of one bit. The first bit of each word in sequence is transmitted, then the second bit of each word, and so on until the frame is complete. Bursts of errors are thus spread out to cause no more than one bit error per word (which is fully correctable) unless a burst persists for longer than 50 ms. Errors in the data from line noise are entirely negligible in practice.

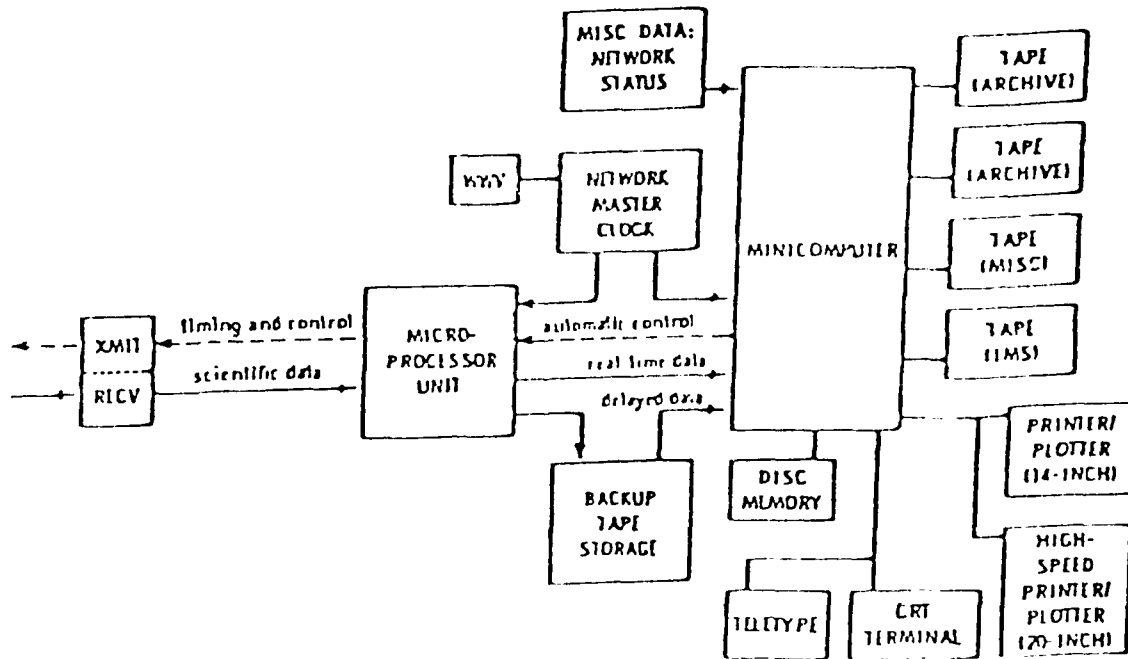
THE COMMUNICATION LINK

The data-acquisition station at AFGL is linked to the data-collection stations by a voice-grade communications network leased from Western Union. The network is full-duplex (i.e. affording simultaneous two-way communication, an outlink and an inlink). It consists of nine segments laid out to form a tree, as shown with AFGL at the base and a DCS at the end of each branch. An outbound signal, therefore, can be sent simultaneously to all of the DCS's, but they must respond in turn. At each hub the first branch with traffic seizes the line and holds it until the transmission is completed.

DATA CONTROL

The functions of the DAS may be grouped in two areas: network control, discussed in this section, and data reception and processing. A schematic representation of the DAS is shown. Ten stations may be accommodated by the communications system. The inlink is used for data return, time shared by all of the DCS's, each of which transmits a frame of digitized data in a programmed sequence. Each DCS responds according to instructions contained in the network-control signal, which synchronizes the taking of data samples by the scientific instruments and the transmission of these data at the proper time. Signal propagation delays are precisely compensated so that sampling times at all stations are simultaneous to within several milliseconds. The details of sampling, storing, and transmitting follow a stored microprocessor program of the DCS.

REPRESENTATION OF DAS



Until the past year, programs which used the data needed to incorporate a means of checking and editing the raw data. This proved to be a very difficult and time consuming activity.

Bedford Research Associates has written a series of computer routines which successfully unpack this very complex data base. Now, for the first time, AFGL scientists have access to processed data with relative ease (with contractor support) and meaningful investigations are now beginning. The project is at a critical phase. Any interruption of support or change in personnel would cause substantial delays for AFGL scientists. While the system is well documented, it is also one that will require many months of time and effort before someone else could be at a stage to even think about using the programs.

This processing capability will be used to generate basic user tapes. These tapes, containing edited data, processed data, will be arranged in compressed blocks covering one minute intervals. The basic user tapes will be made available to the scientific community.

REALTIME DATA

The network minicomputer has the capability of doing some data reduction in real (or near-real) time and automatically providing the results to users via an appropriate communication link. The first such system is under construction; it will provide special 15-minute alerts and 90-minute magnetometer ranges from all stations to the Air Weather Service (AWS) at the Offutt AFB near Omaha, NB, via an existing teletype network. In this system, the minicomputer delivers data every 15 minutes to a fully automated microprocessor-based responder, which constructs formatted messages and transmits them to the AWS computer. It is expected that a realtime detection of sudden commencements and impulses will also be incorporated into this system.

DATA ACCESSING ROUTINE

Since a large data base is being created, a standard routine was envisaged to access any point of the data. This would eliminate any redundant efforts needed to access separate parts of the data in separate analyses. However, detailed consideration was necessary to provide a subroutine which would be easily usable in applications.

The data are read from file MSDATA by functions MGREAD (MSINN, ID, IDATA, NDATA, NSTA). MSINN is the earliest acceptable time in milliseconds since 1970. If positive, the next satisfactory data set is provided. If MSINN is -1, the last data set which was extracted is reused. If a millisecond count is set negative, then only that number of milliseconds or the closest time after that specified is acceptable. If only a particular station is wanted, the negative of the station number is entered in NSTA: positive values are not checked.

The data set is specified by MSINN and possibly NSTA. ID indicates which data are to be extracted from the set.

Of the two decimal digits of ID, the first specifies the type of data, the second subdivides the type. The values 34 and 14 give the vector values of the magnetic field each second and the change in the magnetic field each .2 seconds.

The general requirements defining the main program were flexibility in use, the possibility of expansion and modification and the capability to be used in either batch mode or interactively.

Flexibilities can be obtained through use of the modular structure; each input card specifies a module to be executed. This allows modules to be added or modified individually and puts the ordering of modular operations

under control of the input deck. For ease in interactive use and in batch, the input is free form with a keyword being a mnemonic in the operation to be done. Interactive use restricts the size of the allowed program requiring an overlay structure. The main overlay was defined to be small as possible with a higher overlay to interpret the keyword cards and control the main overlay. This allows the other overlays to be treated as modules. The separate overlays act as individual programs except that (1) certain data can be passed between them or saved and reused and (2) they can link each other without requiring another keyword card.

The data is packed into 12 bit quantities, which will be called slots to avoid conceptual problems with 16 and/or 12 bit words. The slots are grouped into sets; the sets in turn are grouped into records.

The data stored are signed integers in 2's compliment form. A slot may contain a single 11-bit integer, sign and a 10-bit magnitude, plus a flag in the low order bit, which is set if the data is suspect. The initial slots in a set, which contain information pertinent to accessing the data, are 12-bit signed integers; i.e., they do not have a flag as the low order bit. However, a string of data may be compressed into an initial value, a string of deltas (the increment from the present value to the next), and the final value. The compression results from the restriction of the deltas to 6,4,3,2, or 1/bit quantities which are packed into the slots giving packing factors of 2,3,4,6 and 12. The shortened deltas are packed from low order to high which is opposite many conventions. The first delta is inaccurate. To reconstruct the data the deltas must be used in reverse order to produce the data from the next to the last value to the second. In the case of a value remaining constant, no deltas are stored and only one value is stored.

Some slots may contain strings of one-bit flags. In this case the packing is from high order to low.

The first three slots of a data set gives the type of data set, the subtype of data set, and the total number of slots comprising the data set.

A data set has two different formats depending on whether packing was used. The fourth word is set to slots containing the information needed to access the data in the two cases. Brackets, [], indicate data which might be packed. Vector data is given in three arrays: all x-data first, then y, then z. X is north, y is east, and z is down.

Since the records have a maximum length of 2560 slots and the sets of slots have a variable length, a data type of -1 terminates the records. There may be slots filled with garbage after the -1 data type but no data should follow until the next record.

The tape ends with a double end of file, a single end of file, or the physical end of the tape. Since some tapes have been restarted, an end of file may be followed by subsequent data.

In addition to the transmission errors which are detected and either corrected or flagged, errors of various types evidence themselves in the time parameter; among these are: erroneous time, data apparently out of chronological sequence, and subsequent data overwriting the start of a data tape.

PROGRAM STRUCTURE

The program was designed for an overlay structure to save space. The main overlay was designed as simply as possible; its sole function is to call higher overlays upon command and pass data. Significant data is passed via commons as are the commands controlling the calling of overlays.

A few generally useful subroutines are included which are used by several overlays. One results of this organization is that general data read to control one keyword may be available for others even when different overlays are used.

The program was constructed and checked under a system which kept a record of all modifications.

Overlay (1,0)---Control

Overlay (1,0) controls the program. Keyword cards are read in and acted upon. For ease in use these are free field cards modelled after the CDC job control cards, except that numeric fields may be either integer or real. Keywords which change parameters or do simple tasks are acted upon in this overlay. Those needing magnetogram data request the main overlay to call in the appropriate overlays before returning control to this overlay. In this way, the modular structure of the entire program is maintained; control of the sequence of operations is given to the person running the program through the keyword cards.

Overlay (2,0)---Data Base Access

In many ways this overlay does the main task of the program: a data tape is read and a compact data file is created. The data tape, MGDATA, is read by MGREAD as described in section 2.1.1. The data is checked for bad spots while being unpacked and bad data is replaced by 99990. or 99999. (This could be changed through common /MGREADC/). The data times returned are checked if the data is to be used. Times showing jumps greater than 15 seconds are stored until either the time discrepancy resolves itself or the error storage area is filled. In the former case, the times of the saved data is corrected before the data is used; in the latter, the new time is considered correct. Time reversals due to long sections of bad data impede

the use of the following data. For this reason MGDATA is not normally rewound before use so that the tape may be positioned externally from the reading routine.

Once the data has been unpacked and checked for problems, especially time discrepancies, and it is from one of the stations and time interval desired, the data is stored by routine STODTA in the buffer IBUF. When this buffer is full, the routine AVGOUT is called to pack the data into the buffer I0B. The data is packed by averaging controlled by two main parameters: NMSAVG and MSDAVG. NMSAVG is the number of milliseconds to be averaged over. MSDAVG is the displacement from one average to the next. NTAVG AND NTDAVG are the number of time points in the average and in the displacement assuming MSPT milliseconds per time point. Depending on the relative values of these parameters, the averages may overlap producing smoothing or they may be widely separated for sampling. Averaging over one sample results in direct use of the data. Data which was flagged by MGREAD is not used and averages with no data are flagged by AVGFLG, set to 65536. Times having no data are flagged by FFLAG, also set to 65536. Data not needed for further averaging is flushed from the buffer and the remaining data repositioned.

When the output buffer is filled, subroutine I0BUT is called to output the data as a record of file AVGEN and to adjust the buffer parameters to allow more data to be placed in it.

Overlay (3,0)---Plotting

This overlay extracts data from AVGEN and organizes it for plotting. The plotting request can be for any length of time, and for any number of stations. To allow for this flexibility, the routine may break a requested time period into several plots. Each plot is limited to MNP points, currently equal to 720. This may result in sampling the points rather than use all

of them; in this routine, sampling rather than averaging is done.

This overlay and the next can be used interactively to examine sections of the data in as much detail as desired.

Overlay (4,0)---Specialized Storage

This overlay transfers data between the standard file and a random access main storage file. When data is transferred from AVGEN, the two files do not have to agree in their parameters controlling the spacing of data points. Data from AVGEN, falling with the time interval and from the desired stations will be transferred to the position in MSFILE whose time is the closest. When a new AVGEN file is created, its time parameters are derived from thos of MSFILE. To make the file AVGEN more compact, only data from the specified stations are used and only times having at least one valid piece of data are used.

MAGNETOGRAM PROCESSING

0. Introduction

The magnetogram data were collected at seven stations, transmitted to the Air Force Geophysical Laboratory, and stored on magnetic tape. The data from one station consists of readings of the magnetic field of the earth, the rate of change of the field, and some engineering data. This data is collected, packed, and stored for 10 second intervals at each site. The packed data is transmitted in ten second blocks from the station to AFGL. A dedicated mini-computer reorganizes the data and stores it on magnetic tapes. These tapes form the data base.

The stations are listed in Table 1. More detailed information on the magnetometer data network may be found in D.J. Knecht, R.O. Hutchinson, and C.W. Tsacoyeanes, AN INTRODUCTION TO THE AFGL MAGNETOMETER NETWORK, Air Force Geophysics Laboratory, April, 1979. (Unpublished).

The main ideas governing the construction of a routine to read this data base and of a main program to analyze and display the data are given in section 1. Section 2 covers aspects of the analysis program as well as detailed descriptions of the data bases used or created; in particular the structure of the main data base is given in section 2.1.1. Particulars of the use of the program are in section 3.

1. Basic Concepts

1.1 Data Accessing Routine

Since a large data base is being created, a standard routine was envisaged to access any point of the data. This would eliminate any redundant efforts needed to access separate parts of the data in separate analyses. However, detailed consideration was necessary to provide a subroutine which would be easily usable in applications.

The data are read from file MSDATA by function MGREAD, (MSINN, ID, IDATA, NDATA, NSTA). MSINN is the earliest acceptable time in milliseconds since 1970. If positive, the next satisfactory data set is provided. If MSINN is -1, the last data set which was extracted is reused. If a millisecond count is set negative, then only that number of milliseconds or the closest time after that specified is acceptable. If only a particular station is wanted, the negative of the station number is entered in NSTA; positive values are not checked.

The data set is specified by MSINN and possibly NSTA. ID indicates which data are to be extracted from the set.

Of the two decimal digits of ID, the first specifies the type of data, the second subdivides the type. The possibilities are listed in table 1.2. The values 34 and 14 give the vector values of the magnetic field each second and the change in the magnetic field each .2 seconds.

Additional controls are provided through commons. In particular, /MGREDC/ and /STANUM/ provide switches for optional handling of bad data; /MGDIMF/ indicates the present location on the tape and control restarting; /MGDATC/ control the unit read.

1.2 Program Requirements

The general requirements defining the main program were flexibility in use, the possibility of expansion and modification and the capability to be used in either batch mode or interactively.

Flexibility can be obtained through a modular structure where each input card specifies a module to be executed. This allows modules to be added or modified individually and puts the ordering of modular operations under control of the input deck. For ease in interactive use and in batch, the input is free form with a keyword being a mnemonic for the operation to

be done. The interactive use restricts the size of the allowed program requiring an overlay structure. The main overlay was to be as small as possible with a higher overlay to interpret the keyword cards and to control the main overlay. This allows the other overlays to be treated as modules. The separate overlays act as individual programs except that certain data can be passed between them or saved and reused and that they can link to each other without requiring another keyword card.

Location		Geographical		Magnetic		Initial	Dials	Std Index	Data Transmission Index
N Lat	W Long	N Lat	E Long						
48.3	117.1	55.2	299.6	NEW,	WA	WA	1	1	1
44.2	103.1	54.1	317.3	RPC,	SD	SD	2	2	3
44.0	90.3	56.3	334.2	CDS,	WI	WI	3	3	5
42.6	82.9	55.8	344.8	MCL,	MI	MI	4	4	7
42.2	71.3	55.8	1.9	SUB,	MA	MA	5	5	9
17.8	82.5	40.7	344.9	TPA,	FL	FL	6	6	8
34.7	120.6	40.2	300.6	LOC,	CA	CA	7	7	2

MAGNETOMETER STATIONS

Table 1.1

ID	Value	Data Item Every sec.	Total Number of Values
11	x component	search coil	.2
12	y component	search coil	.2
13	z component	search coil	.2
14	Full vector	search coil	.2
21	x component	Fine Flux	1
22	y component	Fine Flux	1
23	z component	Fine Flux	1
24	Full Vector	Fine Flux	1
31	x component	Total Flux	1
32	y component	Total Flux	1
33	z component	Total Flux	1
34	Full Vector	Total Flux	1
41	x component	Coarse Flux	5
42	y component	Coarse Flux	5
43	z component	Coarse Flux	5
44	Full Vector	Coarse Flux	5
51	Additional Data		3
52	Analog Engineering Data		3
54	Digital Engineering Data		3

DATA TO BE EXTRACTED

Table 1.2

2. **Structures**

The main structures are given in this section

2.1 **Data Structures**

2.1.1 **Magnetogram Data Tapes**

The standard file name for these is MGDATA. The tapes are 7 track, 800 b.p.i. A short description of the format is given below; for a complete description, see D.J. Knecht, Archive Data Tapes of the AFGL Magnetometer Network, Air Force Geophysical Laboratory, to be printed (Unpublished).

The data are packed into 12 bit quantities, which will be called slots to avoid conceptual problems with 16 and/or 12 bit words. The slots are grouped into sets; the sets in turn are grouped into records.

The data stored are signed integers in 2's compliment form. A slot may contain a single 11-bit integer, sign and 10-bit magnitude, plus a flag in the low order bit, which is set if the data is suspect. The initial slots in a set which contain information pertinent to accessing the data, are 12-bit signed integers; i.e. they do not have a flag as the low order bit. However, a string of data may be compressed into an initial value, a string of deltas (change from the present value to the next), and the final value. The compression results from the restriction of the deltas to 6,4,3,2, or 1 bit quantities which are packed, the slots giving packing factors of 2,3,4,6, and 12. The shortened deltas are packed from low order to high, which is opposite many conventions. The first delta is inaccurate. To reconstruct the data the deltas must be used in reverse order to produce the data from the next to the last value to the second. In the case of a value remaining constant, no deltas are stored and only one value is stored.

Some slots may contain strings of one-bit flags. In this case the packing is from high order to low.

The first three slots of a data set define the type of data set, the subtype of data set, and the total number of slots comprising the data set.

A data set has two different formats depending on whether packing was used. The ordering of the data is described in Table 2.1. The fourth word is set to 1 if packing was used and to -1 if it was not. The two columns of slot numbers in Table 2.1 indicate which slots contain the information needed to access the data in these two cases. Brackets [], indicate data which might be packed. Vector data is given in three arrays: all x data first, then y, then z. X is north, y is east, and z is down.

Since the records have a maximum length of 2560 slots and the sets of slots have a variable length, a data type of -1 terminates the record. There may be slots filled with garbage after the -1 data type but no data should follow until the next record.

The tape ends with a double end of file, a single end of file, or the physical end of the tape. Since some tapes have been restarted, an end of file may be followed by subsequent data.

In addition to the transmission errors which are detected and either corrected or flagged, errors of various types evidence themselves in the time parameter; among these are: erroneous time, data apparently out of chronological sequence, and subsequent data overwriting the start of the data tape.

TABLE 2.1 DATA FORMATS

Packing Used Slot	No Packing Slot	Quantity
1	1	1 (type)
2	2	0 (subtype)
3	3	Number of slots
4	4	Packing flag: 1 = packing -1 = no packing
5,6,7	/	No. of bits/value for Search Coil X,Y,Z
8,9,10	/	No. of bits/value for Fine Flux X,Y,Z
11,12	/	No. of bits/value for Analog and Digital data
13,14	5,6	Time of receipt of data in seconds past 10 second mark and milliseconds
15	7	Diagnostic check for mini- computer
16, on 8, on		Actual data:
		[Search Coil X] 50 values of each [Search Coil Y] Unit=gamma/sec [Search Coil Z]
		[Fine Flux X] 10 values of each [Fine Flux Y] Unit=gamma/sec [Fine Flux Z]
		[Coarse Flux X] 3 slots for each [Coarse Flux Y] 2 values, unit = 64 [Coarse Flux Z] Flag string, align with fine flux value indicating location of change
		[Analog data] 23 values [Digital data] 15 values
	Additional data	13 slots
	1	5 volt values
	2	Temperature of electronics
	3	Temp. of sensor
	4	Station ID number
	5	Serial Number
	6,7	Status words
	8,9,10	Synch words
	11,12,13	Time of data

2.1.2 Averaged General Data File

The file AVGEN is the main file for data use. Overlay (2,0) creates this file from the data tapes. (4,0) transfers data between this type of file and mass storage. (3,0) plots data stored on AVGEN. The file OLDAVG has the same structure.

The first logical record is a character string labeling the file. The first 100 characters contain the date and time which the file was created as a standard file. Subsequent sets of 10 characters contain the date and title of each run which modifies the file. A list of abbreviations of the stations used end the record.

The second logical record consists of data specifying the averaging and packing of the magnetic data held on the file. This consists of copies of the two commons /AVGC/ and /STATC/. Each copy is preceded by one word giving the length of the common; this allows for future changes without invalidating any earlier files. The data in the commons are described individually in the description of overlay (2,0).

The following logical records consist of as many sets as can fit into LI0B words; LI0B being set to 512. A set consists of a time word and three average data words from each station which is to be included. Thus, if NSTA stations are used, a set has $3 * \text{NSTA} + 1$ words. The time word is an integer giving the average time in milliseconds since 1970. The data words are the average flux with the value of AVGFLG, set to 65536., indicating the lack of data.

The data are in chronological order. The number of points per average is NTAVG and the spacing of averages is MSDAVG; thus the average could contain one point for non-averaging, could overlap for smoothing, or could be widely separated for sampling. The parameters may be changed by input cards.

2.1.3 Mass Storage Data File

The file MSFILE is a random access storage file which allows large amounts of data to be stored and accessed easily. The data must be put into AVGEN form before using but this can be done quickly and without imprinting a tape.

The file is a CDC random access file with a numerical index. The first record is a character string containing the starting and ending date and time, a general label, a list of station initials, and the date, time and title of each run contributing to the file.

The second record contains a copy of common /RAMXS/. The contents are described in detail in the section on overlay (4,0).

The other records contain data. The first word is the time of the first data set. Each record contains data sets each of which has NQSETM items: NDSM items from each of NSTAM stations. The time interval between sets is MSDMS milliseconds. The time of the first data set is given in milliseconds since 1970. If a datum is absent the value FILLMS, set to 65536., is used. Each record contains an interval of MSREC milliseconds and the initial record starts at INTMSM milliseconds since 1970.

2.2 Program Structure

The program was designed in an overlay structure to save space. The main overlay was designed as simply as possible; its sole function is to call higher overlays upon command and pass data. Significant data are passed via commons as are the commands controlling the calling of overlays. A few generally useful subroutines are included which are used by several overlays. One result of this organization is that general data read to control one keyword may be available for others even when different overlays are used.

The program was constructed and checked under a system which kept a record of all modifications. Since this system is of more general use it is described in appendix A.1.

The overlays are described in the following sections. The routines are listed in tables 2.2.nR and the commons in table 2.2.nC where n is the number of the overlay. Similarly, flow charts of the main routines are in figures 2.n.

2.2.1 Overlay (1,0) --- Control

Overlay (1,0) controls the program. Keyword cards are read in and acted upon. For ease in use these are free field cards modeled after CDC job control cards, except that numeric fields may be either integer or real. Keywords which change parameters or do simple tasks are acted upon in this overlay. Those needing magnetogram data request the main overlay to call in the appropriate overlays before returning control to this overlay. In this way, the modular structure of the entire program is maintained; control of the sequence of operations is given to the person running the program through the keyword cards.

2.2.2 Overlay (2,0) Data Base Access

In many ways this overlay does the main task of the program: a data tape is read and a compact data file is created. The data tape, MGDATA, is read by MGREAD as described in section 2.1.1. The data is checked for bad spots while being unpacked and bad data is replaced by 99990. or 99999. (This could be changed through common /MGREDC/). The data times returned are checked if the data are to be used. Times showing jumps greater than 15 seconds are stored until either the time discrepancy resolves itself or the error storage area is filled. In the former case, the times of the saved data is corrected before the data is used; in the latter, the new time is considered correct. Time reversals due to long sections of bad data impede the use of the following data; for this reason MGDATA is not normally rewound before use so that the tape may be positioned externally from the reading routine.

Once a data set is unpacked and checked for problems, especially time discrepancies, and it is from one of the stations and time interval desired, the data is stored by routine STODTA in the buffer IBUF. When this buffer is full, the routine AVGOUT is called to pack the data into the buffer IOB. The data is packed by averaging controlled by two main parameters: NMSAVG and MSDAVG. NMSAVG is the number of milliseconds to be averaged over. MSDAVG is the displacement from one average to the next. NTAVG and NTDAVG are the number of time points in the average and in the displacement assuming MSPT milliseconds per time point. Depending on the relative values of these parameters, the averages may overlap producing smoothing or they may be widely separated for sampling. Averaging over one sample results in direct use of the data. Data which was flagged by MGREAD is not used and averages with no data are flagged by AVGFLG, set to 65536. Times having no data are flagged by FFLAG, also set to 65536. Data not needed for further averaging is flushed from the buffer and the remaining data repositioned.

2.2.3 Overlay (3,0) Plotting

This overlay extracts data from AVGEN and organizes it for plotting. The plotting request can be for any length of time, and for any number of stations. To allow for this flexibility, the routine may break a requested time period into several plots. Each plot is limited to MNP points, currently equal to 720. This may result in sampling the points rather than use all of them; in this routine, sampling rather than averaging is done.

This overlay and the next can be used interactively to examine sections of the data in as much detail as desired.

2.2.4 Overlay (4,0) Specialized Storage

This overlay transfers data between the standard file and a random access main storage file. When data is transferred from AVGEN, the two files do not have to agree in their parameters controlling the spacing of data points. Data from AVGEN, falling within the time interval and from the desired stations will be transferred to the position in MSFILE whose time is the closest. When a new AVGEN file is created, its time parameters are derived from those of MSFILE. To make the file AVGEN more compact, only data from the specified stations are used and only times having at least one valid piece of data are used.

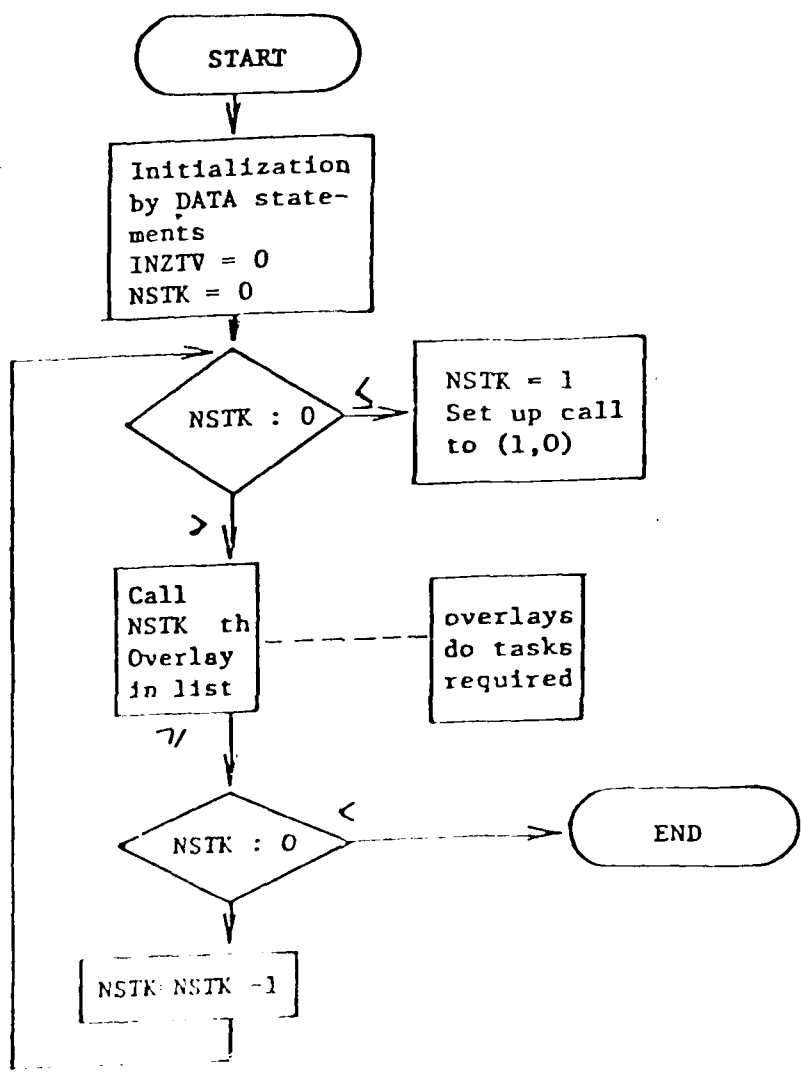


FIGURE 2.0
Overlay (0,0) Base Overlay

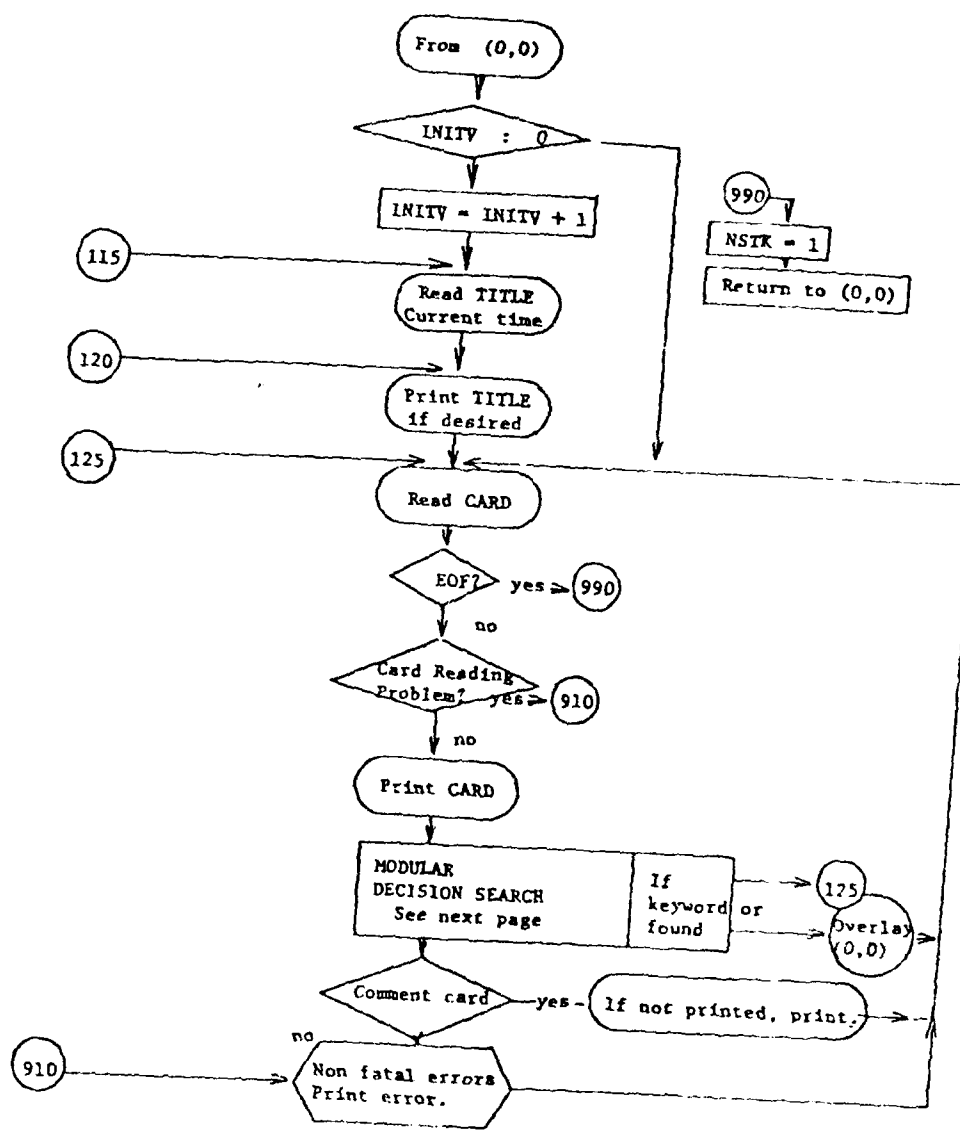


FIGURE 2.1
Overlay (1,0) Standard Modular Driver/controller

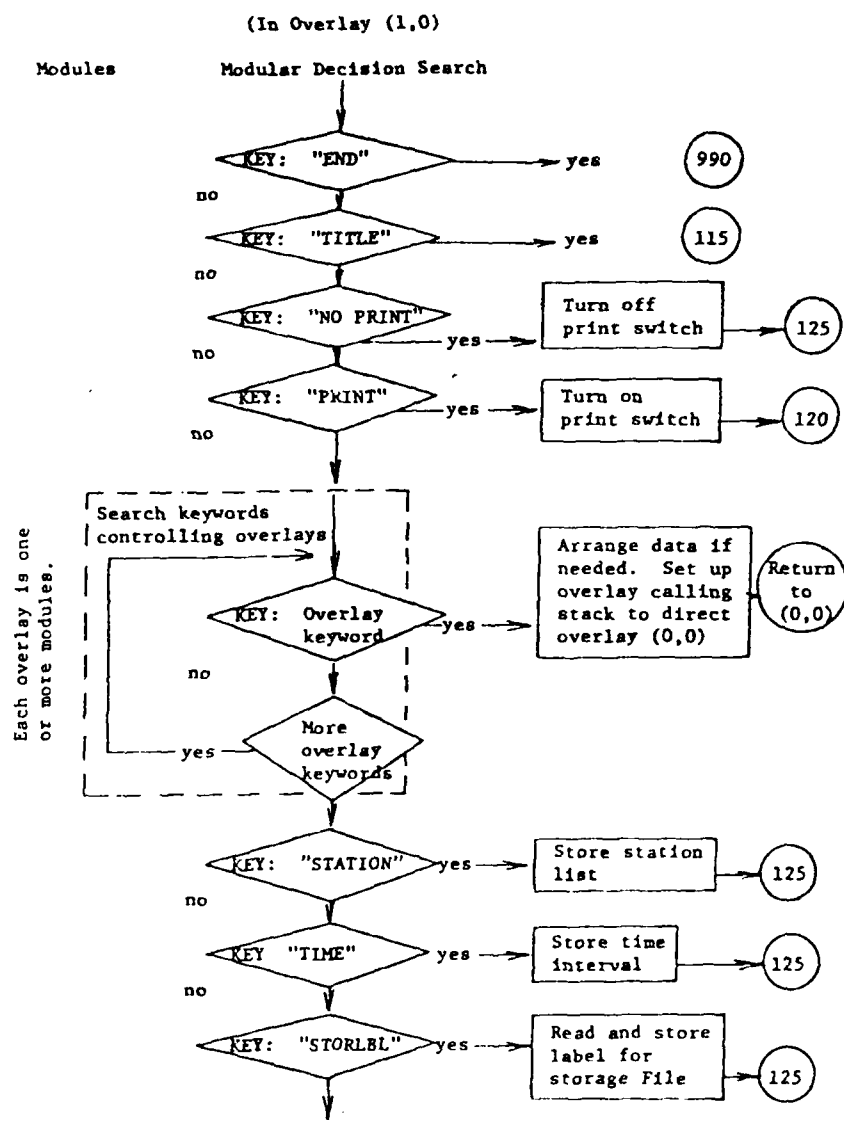
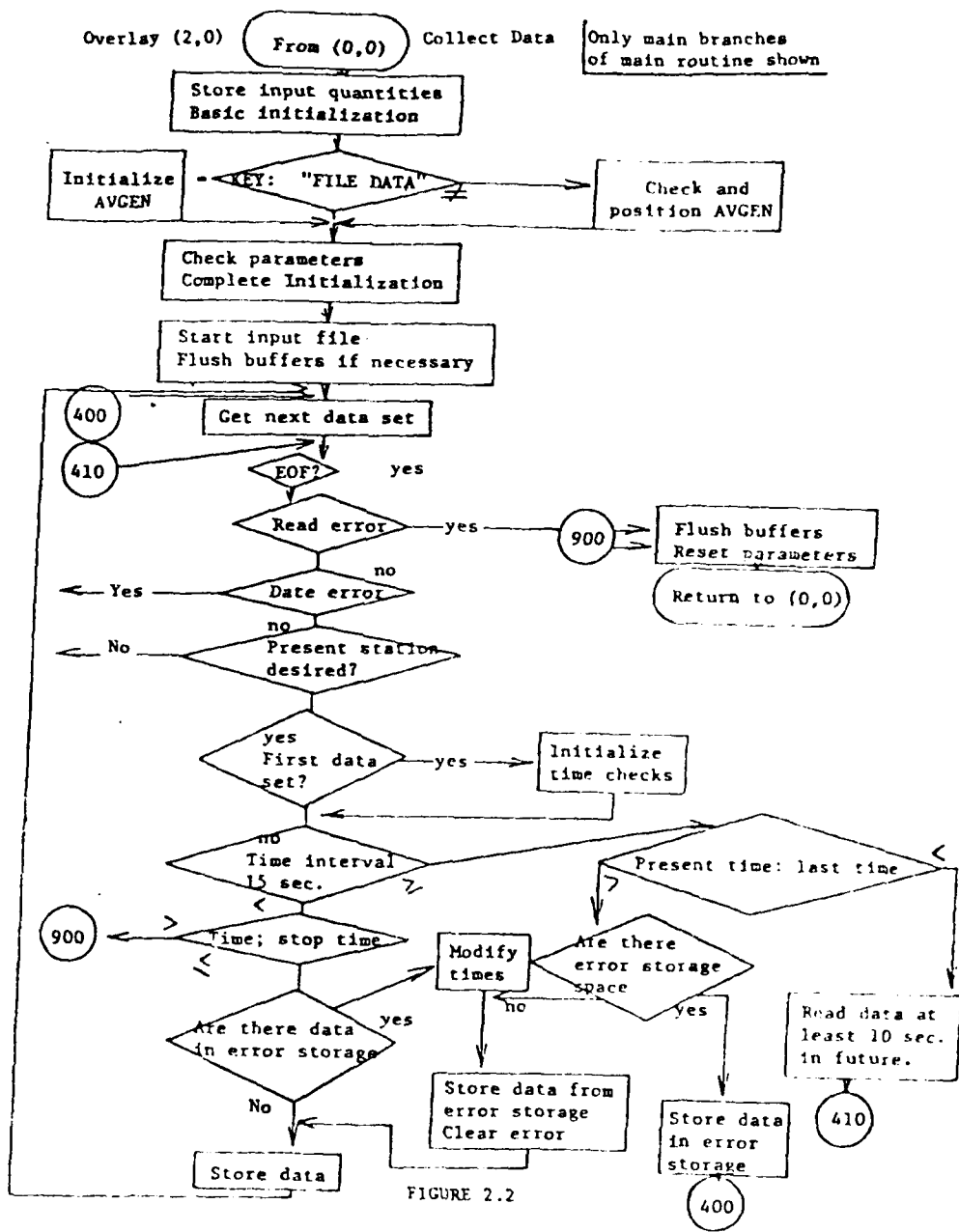


FIGURE 2.1.1



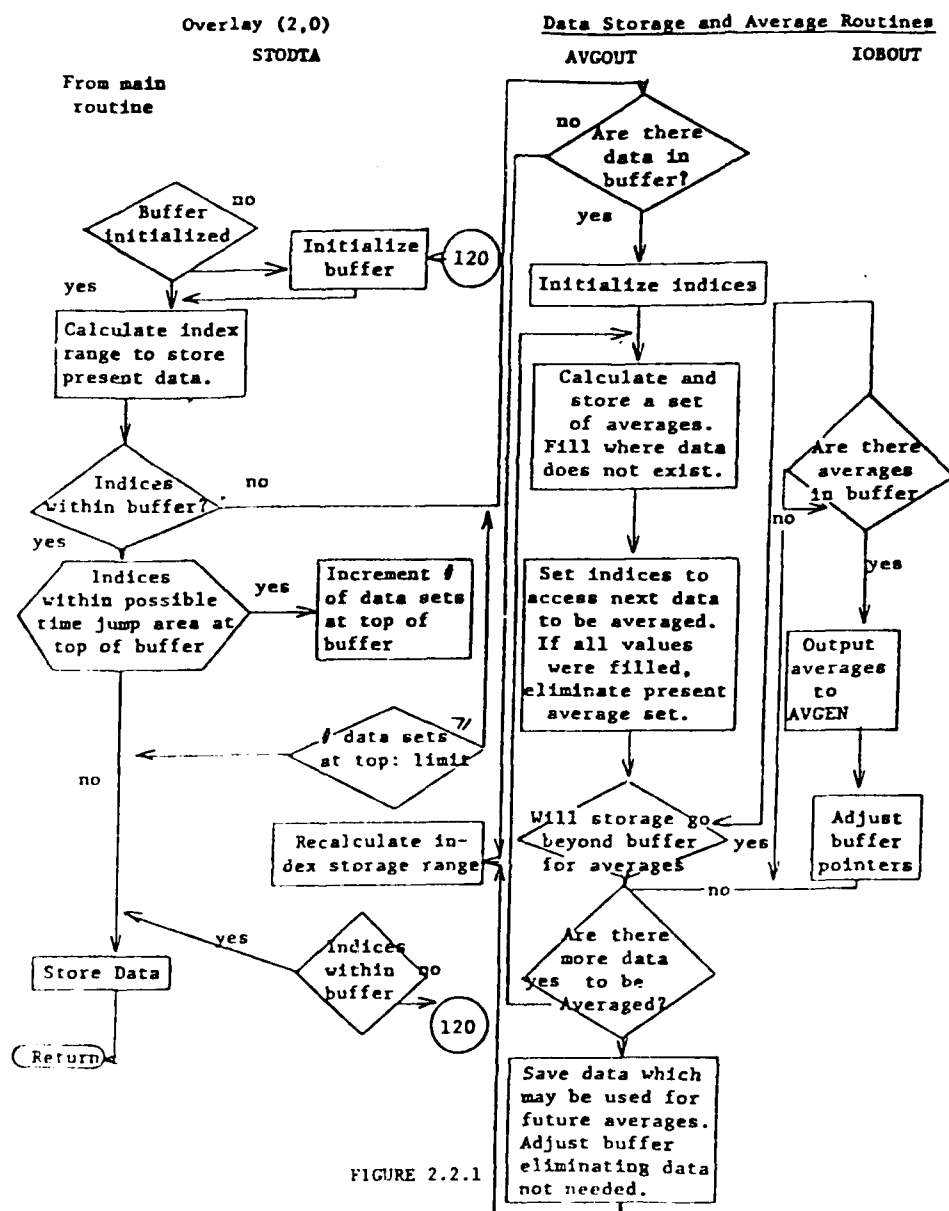


FIGURE 2.2.1

Overlay (3.0)

Plotting Overlay

(From 3.0)

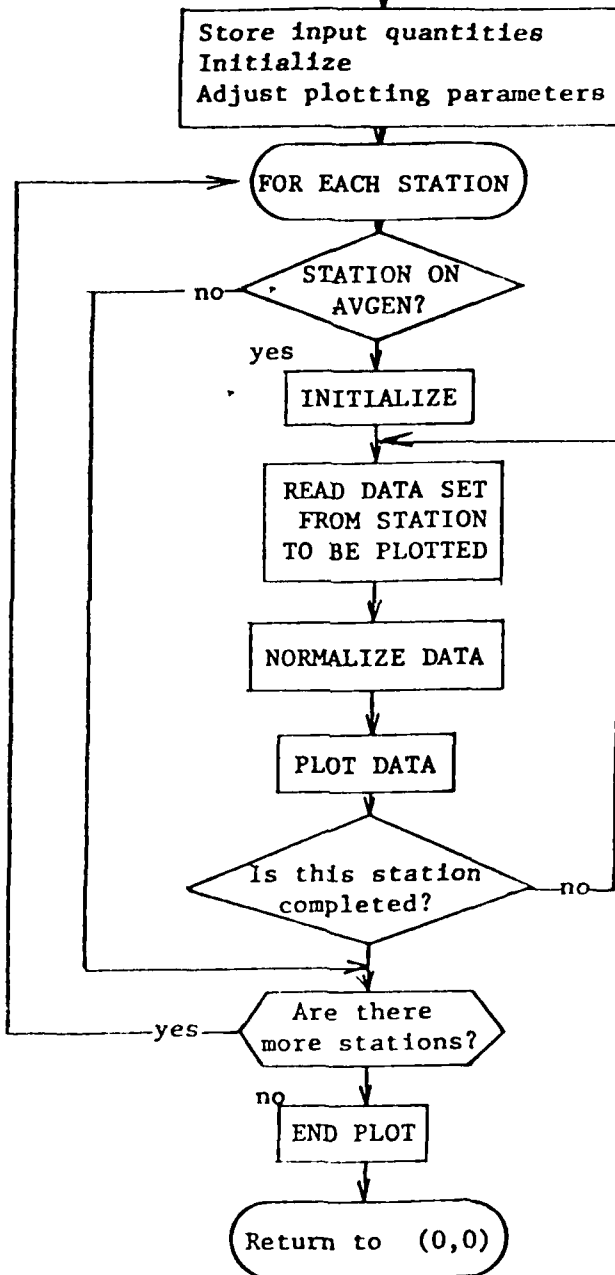


FIGURE 2.3

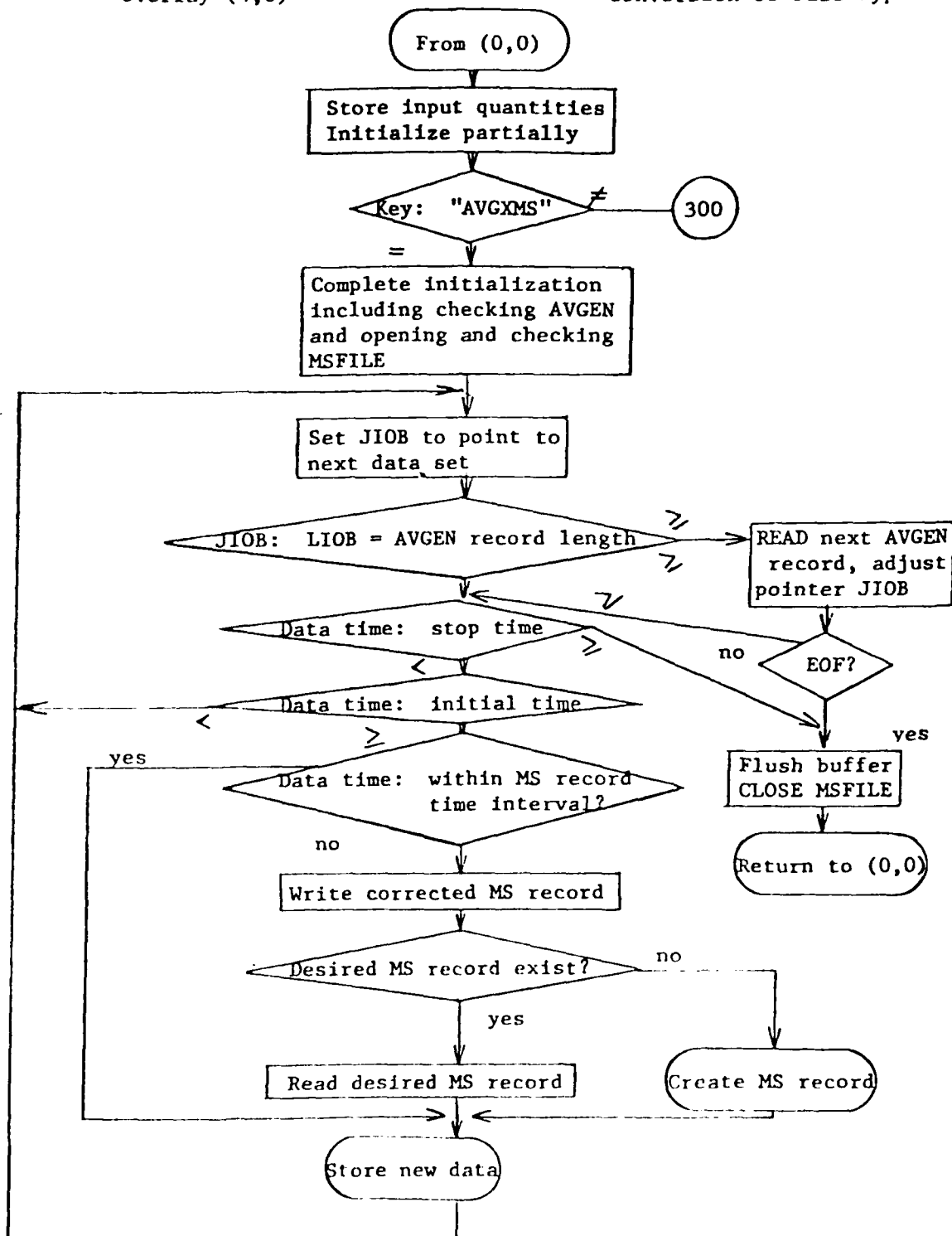


FIGURE 2.4

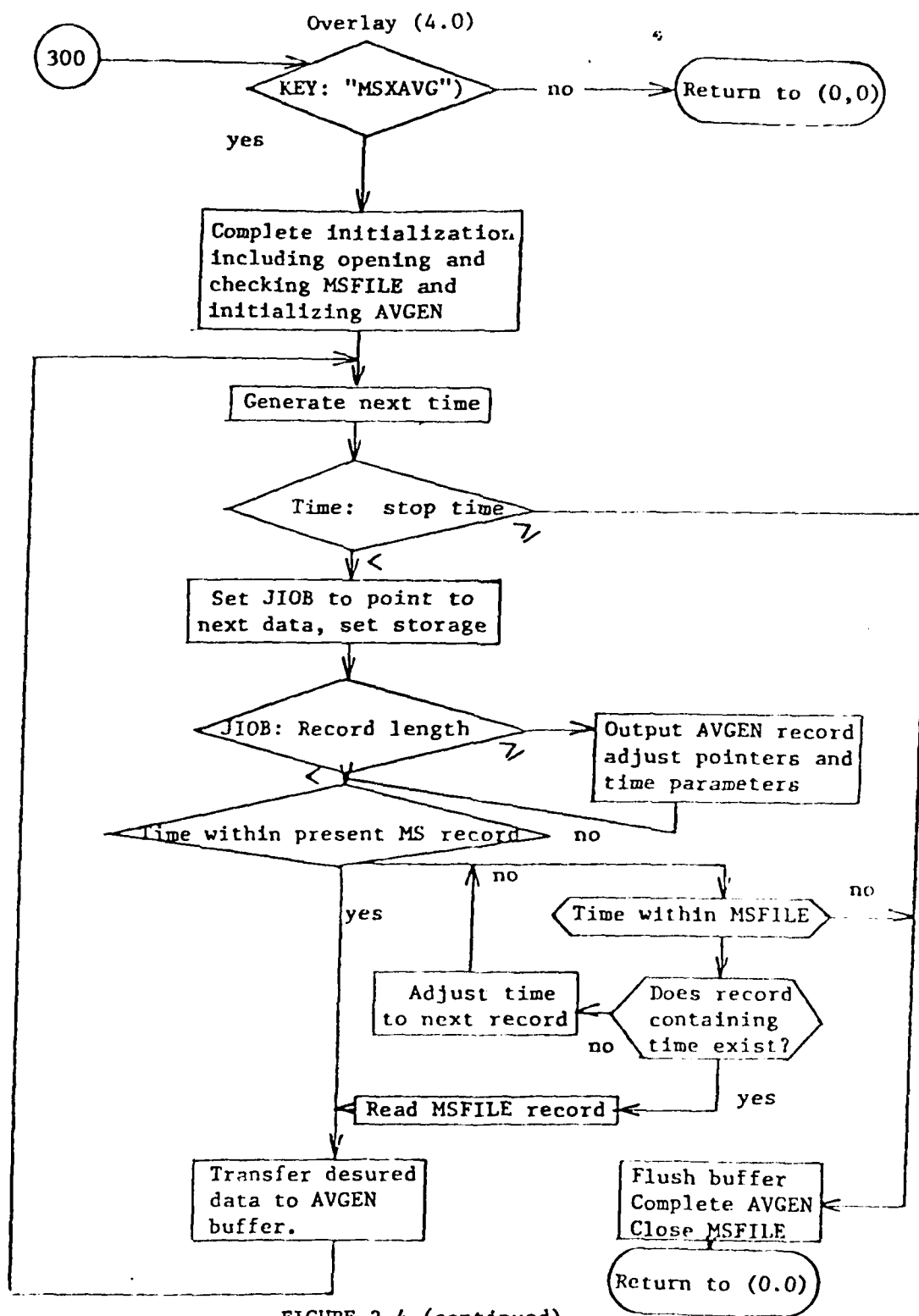


FIGURE 2.4 (continued)

A.2 Special Programs

Three routines were developed to aid in checking the files. The first is currently useful in checking data problems while the latter two routines are useful in checking the contents of the files.

DUMPMG prints records from the archive tapes. The data is printed on octal just as it is received by the CDC 6600 and must be interpreted manually. This allows data problem areas to be checked in detail.

PFPRNT prints the contents of the file AVGEN. The number of CDC words in each record is given. The label and access data records are listed. For each data record, the times and corresponding data are listed in tabular form. The time is given in the concatenated form as well as milliseconds since Jan. 0, 1970.

DMPMS prints a summary of the data in the file MSFILE. The label record is listed. For each record containing data, the range of times covered by that record are listed. The data itself is not checked so that gaps within the time intervals are not noted.

Further development might include the incorporation of these routines into MGOVL and expanding their capabilities. It would be helpful if AVGEN and MSFILE could be scanned in detail, within particular times or in total, and all data gaps larger than a particular value be reported for all stations or for selected ones.

/OVERLAY/	Defines KEYWORD - Overlay Relation
NOVL 10	Number of overlays
MOVL 16	Max. number of overlays
NDOVL 5	First dimension of KOVL
KOVL (5,16)	Keyword overlay array, 1st index
/SOVRLY/	Sequential Overlay Link
KSTK 0	Index for KSTK for next overlay after decrement
MSTK 8	Max. number overlay links
NSTK (8)	Overlay link stack
/INITOV/	Initialization Switch
INITV 0	First card is read as title if INITV is 0
/IO/	I/O Common
IN	Input file
IOUT	Output file
/IOX/	I/O Extra Files
IOLD	Old AVGEN to be copied from
IAG	General average data file
MSF	Mass storage file
/MGDATA/	Data Input File
MGDATA 6LMGDATA	Magnetometer Archive Data Tape
/KEY/	Keyword common
NZ	Number of items
MZ 12	Max. number of items
KEY	Keyword
IZ (11)	Other items from card
KKEY	Keyword key
K7 (11)	Keys indicating formats used for interpreting IZ
/EQUIV/	Equivalence Common
NEQ 3	Number of defined parameters
MEQ 8	Max. number of parameters
IEQ(8) 0	Values obtained from card
NKQ(2,8)	Symbol definition/expected key

TABLE 2.2.OC

COMMONS IN BASE OVERLAY

		STA numerical (real) Station string
		DEL numerical (real) Output data step
		ASEC numerical (integer) Number seconds average
/CARD/		Keyword card common
MCARD 80		Number of columns used
KARD(80)		Card characters
/TITLEC/		Run Title Common
DATE(2)		Date and time when title was read
TITLE(8)		Title from title card
/PRTST/		Print Switch
PRTEST		Printing to be done?
/STLBLC/		Storage Label Common
STLBL(8)		Label for data set
/TIMEC/		Title Common (*means initialized by MTIME)
INTC 0		Initial time concatenated
INTDAY *		Days since 0 Jan. 1970
INTIME *		Milliseconds in day
INTMS *		Milliseconds since 0 Jan. 1970
LSTC		Last time concatenated
LSTDAY *		Days since 0 Jan. 1970
LSTIME *		Milliseconds in day
LSTMS *		Milliseconds since 0 Jan. 1970
/STATC/		Station Common (*means initialized by STATNS D means initialized by data statement)
ND 3		Number of data/quantities/station/time point
NQT		Number of quantities in time point
KSTA		Station sequence number
JSTA		Data station number
NSTA		Number of stations
MSTA 10		Max. number of stations
LBLOST(10) D		Label external index

IDOST(10)	D	Data index (external index)
LBLDST(10)		Label (data index)
IODST(10)	1	External index (data index)
ISOST(10)	*	Storage index (external index)
ISDST(10)	*	Storage index (data index)
IDLSST(10)	*	Label (storage index)
IOSST(10)		External index (storage index)
IDSST(10)		Data index (storage index)
 /LIOBUF/		Length of Arrays Stored in AVGEN
LIOAVG	69	Length of /AVGC/
LIOST	96	Length of /STATC/
 /PLOTC/		Plot Parameters
I PLOT	-1	Type of plot
MMM	0	Plot Parameter
MAX	1	Plot Parameter
NP	720	Number of points plotted
START		Start time
PLOTIM	24	Plot time (hr)
MSPLOT		Plot time (ms)
DEL	2.	Point spacing (min)
MSDEL		Point spacing (ms)
DELTIC	2.	Time between tics (hr)
 /PLTLBL/		Label for Plot
PLOTID(3)		Label set by data statement
 /SF/		CRT Plot Initialization Parameter
SF	1.5	Plotting scale factor
XP	.5	X - plotting frame value
YP	.5	Y - plotting frame value
 /INTERC/		Common for Interactive Use Parameters
KINTER	0	If non-zero, adjust for interactive operation.

/DATAK/		Buffer to Handle Data Quantities
NDATA	30	Length of data
DATA(30)		Data buffer
/OOPSC/		Buffer for problem data
MSOK	1500	Acceptable millisecond change interval
NDOOPS		Storage needed for one data set plot information
IOOPS		Next error index to be used
LOOPS	96	Error buffer length
KOOPS(96)		Error buffer
/BUFX/		Quantities Defining Buffer Status
MSBASE	-1	First time in buffer (ms), used to calculate index
MSPT	1000	Milliseconds/time point
MSSET		Milliseconds/data set
MPSET	10	Number of time points/data set
NQS	3	Number of data quantities/station point
NQST		Number of quantities/output set
NQSET		Number of quantities/input set
/FFG/		Error Flags
FFLAG	65536.	Fill flag when there is no data
XFLAG	32768	Data greater than this value not used
AVGFLAG	65536.	Value used if there are no points in average
/AVGC/		Quantities Defining Averaging
NMSAVG	=MSTP*NTAVG	Milliseconds averaged over
NTAVG	10	Time points averaged over
MSDAVG	=MSTP*NTDAVG	Millisecond shift between averages
NTDAVG	10	Time point shift between averages
LAVBUF	=NQST*NTAVG	Storage needed for one set of averages
IDAVBF	=NQST*NTDAVG	Index range for one set of averages
MN		Min index for quantities being averaged
MX		Max index for quantities being averaged
NS2	60	Composite dimension of S and XN
S(30)		Sums
XN(30)		Number of items in each sum

TABLE 2.2.2C

ADDITIONAL COMMONS IN OVERLAY (2.2)

/MGDIMF/	See MGREAD for explanation. NREC set to 0 for proper restart	
//	Large buffers	
IOB(512) IBUF(7680)	Final output buffer Buffer to hold data before averaging	
/IOBUFK/	Quantities Defining Buffers	
JJOB	IOB storage index	
LJOB	IOB length	
ISX	IBUF storage index	
LBUF	IBUF length	
LIMISX	IBUF storage limit causing averaging when crossed by initial item of a set	
NISX	Number of times ISX crossed LIMISX	
MISX.	Max. number of times LIMISX may be crossed before mandatory flushing of buffer.	
/BMBFIL/	Data to be Printed at Bombout	
LMS	Last time processed in milliseconds	
<u>CONSTANTS</u>		
IDT	34	Data type wanted from MGREAD
MSMDIF	200000000	Max. forward time jump processed in milliseconds.

//		Plotting Arrays
HDZGAM	(720,3)	Components of magnetic field at different times
XTIME	(720)	Corresponding times
DYGAM	(3,7)	Half-range sizes
BSLV	(3,7)	Mid-range values
/FFC/		Error Flags (Same as in overlay (2,0))
FFLAG	65536.	Fill flag when there is no data
XFLAG	32768.	Data greater than this value is not used
AVGFLAG	65536.	Value used if there are no points in average
/AVGC/		Quantities Defining Averaging (As in overlay (2,0))
NMSAVG		Milliseconds averaged over
NTAVG	10	Time points averaged over
MSDAVG		Millisecond shift between averages
NTDAVG	10	Time point shift between averages
LAVBUF		Storage needed for one set of averages
IDAVBF		Index range for one set of averages
MN		Min. index for quantities being averaged
MX		Max. index for quantities being averaged
NS2	60	Composite dimension of S and XN
S(30)		Sums
XN(30)		Number of items in each sum
/PLOTMS/		Plot Times Common
INPC		Initial time, concatenated, from data set of card
INPDAY		, day
INPTIM		, ms within day
INPMMSM		, ms since 0 Jan., 1970
LSPC		Last time, concatenated, from MSXTRA of card
LSFDAY		, day
LSPTIM		, ms within day
LSPMSM		, ms since 0 Jan., 1970
JPTC		Ongoing plot time, concatenated
JPTDAY		, day
JPTIME		, ms within day
JPTMS		, ms since 0 Jan., 1970

TABLE 2.2.3C

ADDITIONAL COMMONS IN OVERLAY (3,0)

/PLTERR/		Error Check Common
PLTXIN	65536.	Defines errors
PLTXOU	99999.	Value used for errors
/INBUFC/		Input Buffer Common
MIOB	512	Buffer size
IOB(512)		Buffer
/AGLBLC/		Avgen Label Common
LAGLBL	20	Length
IAGLBL(20)		Label
/RED3WC/		Lindage Needed for Restart
MVIRG		

/FFC/		Error Flags (same as in overlay (2,0)
FFLAG	65536.	Fill Flag when there is no data
XFLAG	32768.	Data greater than this value not used
AVGFLAG	65536.	Value used if there are no points in average
/AVGC/		Quantities defining averaging (as in overlay (2,0)
NMSAVG		Milliseconds averaged over
NTAVG	10	Time points averaged over
MSDAVG		Millisecond shift between averages
NTDAVG	10	Time point shift between averages
LAVBUF		Storage needed for one set of averages
IDAVBF		Index range for one set of averages
MN		Min index for quantities being averaged
MX		Max index for quantities being averaged
NS2	60	Composite dimension of S and XN
S(30)		Sums
XN(30)		Number of items in each sum
/RAMSX/		Parameters Defining Random Mass Storage
INTCM		Initial time concatenated
INTMSM		Initial time milliseconds
LSTCM		Final time concatenated
LASTMSM		Final time milliseconds
NSDM (3)		Data items per stations
NSTAM (7)		Number of stations
IMOST		Conversion of standard index to mass storage index
NOSETM (21)		Number of quantities per time set
NTREC	180	Number of time sets per record
MSDMS	120000	Milliseconds per time set
MSREC		Milliseconds per record
LRECMS (3780)		Length of mass storage record file
LRAMSX	44	Length of saved common
LRECMS (3781)		Length of mass storage record
FILLMS	65536.	Fill value

TABLE 2.2.4C

ADDITIONAL COMMONS IN OVERLAY (4,0)

SEARCH	Searches for proper keyword.
NOW	Obtains date and time in characters.
KREAL	Creates real and integer numbers from input character string.
PRTITL	Prints title, time, and page numbers.
IEQUIV	Scans input for equal signs and substitutes.
NUMCVT	Converts between real and integer if necessary.
KEYWRD	Reads and interprets free field input.
HOLLER	Creates Hollerith "values" from input character string.

TABLE 2.2.1R

ROUTINES IN OVERLAY (1,0)

FILDTA	Extracts data from data base and stores it.
MSTOTAL	Converts time to milliseconds.
MGREAD	Extracts desired data.
ISEARCH	Positions data base.
ADDFLUX	Combines flux data which is stored separately in base.
MOVEIT	Adjusts data in double buffers.
MGUNPK	Unpacks packed data.
ISLOTER	Finds next data set.
ITISUM	Extracts time from data.
CHECK	Checks data error flags.
TIMSTOP	Adjusts time parameters to handle time skips.
STODTA	Stores desired data in buffer.
AVGOUT	Averages data, stores average.
IOBOUT	Outputs averaged data and adjusts buffer.
BMBOUT	Is called if system terminates program.
IFCLC8	Finds I/O file list.
NOW	Obtains date and time in characters.

TABLE 2.2.2R

ROUT' > IN OVERLAY (2,0)

MGOVL	Main routine, calls overlays.
STATNS	Initializes station index tables.
MSTIME	Converts concatenated time to milliseconds.
ICTIME	Converts milliseconds to concatenated time.
MOVE	Efficiently moves blocks of data.
INTGRS	Separates number into digits.
IORDR2	Orders a list and adjusts associated list.

TABLE 2.2.OR

ROUTINES IN BASE OVERLAY

//	Buffers
IOB (512)	Avgen buffers
MSX (1536)	Msfile index
MSB (4096)	Msfile buffer
/MSBUFK/	Buffer access parameters
L1OB	Current length of avgen buffer
LMSX	Current length of msfile index
LMSB	Current length of msfile buffer
J1OB	Current index of avgen buffer
JMSX	Current index of msfile index
JMSB	Current index of msfile buffer
/MSLBLK/	Initial label for msfile
MSLBL (10)	Initial label for msfile

SPECGRM	Controls plotting of data from AVGEN.
IRED3W	Extracts data to be plotted.
BASE	Scans data and sets normalization parameters.
MSPLOT	Plots three magnetic quantities.
AAXIS	Writes axis numbers
DAMOYR	Labels plot from concatenated time.
LINER	Plots data.

TABLE 2.2.3R

ROUTINES IN OVERLAY (3,0)

FILCVT	Converts data between files.
INITMS	Initializes mass storage file, MSFILE.
INITAG	Initializes AVGEN.
NOW	Obtains date and time in characters.

TABLE 2.2.4R

ROUTINES IN OVERLAY (4,0)

3. Program Use

This program, MGOVL, is designed to be run either interactively or in batch mode. The program is structured such that the loader under the CDC NOSBE system will create a disk file with a local name MGOVL. This disk file can be made permanent. The program has been restricted to less than 600000 words of memory in order to be run interactively. The running time may be rather long, 650 sec, if entire tapes are processed. The usual tasks done interactively use much less time although it is desirable to raise the default interactive time limit.

A description of the input is given in section 3.1. The current options are listed in section 3.2.

3.1 Input Structure

The input described below is a free field input which is used for both batch and interactive use. A card in batch input is equivalent to a line in interactive use.

The first card read is saved as a title card and used to label the first page of output. The remaining cards are either keyword cards or cards which follow the keyword card requiring them. Each keyword causes values to be stored or an action to be performed. The main inter-dependence is the use by one keyword of values set by an earlier keyword. The program will stop upon reading an END card or an end of record.

The keyword cards are free field cards. The fields are separated by the break characters "," , "(" , and "=" . Leading and trailing blanks are ignored. Scanning ends when a termination character, either ")" or "." plus 20 blanks, or the end of the card is found.

A field with just digits and possibly a preceding sign is treated as an integer. A real number occurs in a field with a point and/or an E preceding an integer field. All other fields are alphanumeric and their first ten characters are used starting with the first non-blank. Blanks will not be removed from within the field but will be added to the end if necessary. After a termination character, the rest of the card can be used for comments. A null field, no non-blank character between two breaks or beyond the termination, usually results in defaults being used. The fields bracketing an "=" may form an equivalence pair. If the first field can be identified, the second field is used and both fields are removed from the card image. If the first field cannot be identified, "=" acts as a standard break character. If the value after the "=" is numeric, the program will convert it to the proper form. This is not true in general. The following are the current equivalence keys:

STA = concatenated list of standard indices for the stations to be processed. The default is all stations.

DEL = minutes between output data points or averages. The default is 1/6 minutes or 10 seconds.

ASEC = seconds to be averaged over. The default is 10 seconds.

If a keyword cannot be identified, an error message is printed and the next card is read. If the first column of the card contains a "C" and no keyword can be identified, it is assumed to be a comment card labelling the input.

3.2 Keyword Definitions

The present keywords and their fields are defined on the following pages. If the card is terminated before all fields are defined, those not defined will be treated as null fields. The keyword is given in upper case; the following fields in lower case.

The concatenated time used for many keywords is an integer in the form: YYDDDDHHMMSS with YY, years since 1970; DDD, Julian day within year; HHMMSS, hours, minutes, and seconds within day.

TITLE Reads next card as a new title.
 NOPRINT Stops printing of input cards.
 PRINT Starts printing of input cards. This is the default.
 END Stops execution. An end-of-record or end-of-file will also halt the program.
 STATION (Station index, station index, station index,...station index).
 Initializes station list based on standard indices; see Table 1.1. This function is also done by equivalence key "STA"; see section 3.1.
 TIME (Initial concatenated time, final concatenated time) Sets time parameter for processing).
 STORLBL Reads next card as a new title for AVGEN file. The default title is "MACNETOMETER NETWORK DATA. FIRST RECORD CONTAINS PACKING AND AVERAGING DATA."
 FILEDATA (Initial time-concatenated, final time-concatenated)
 Initializes AVGEN and outputs data found on MGDATA between the times requested and from the stations requested and averaged as specified. See the equivalence keys in section 3.1.
 ADDATA (Initial time-concatenated, final time-concatenated)
 Positions AVGEN to allow averaged data to be transferred to it from MGDATA starting at the initial time. The status and averaging parameters are determined by those previously used for AVGEN.
 PLOTLBL Reads the first thirty columns of the next card to be the plot identifier. The default is "FOUGERE X3827 MAGNETOGRAM".
 INTER Causes the program to stop before and after each plot for interactive control.
 NINTER Causes the program to continue through the plots. This is the default.
 SF (Scale factor) Sets the plotting scale factor. If null, it is reset to default 1.5.
 PORG (x,y) Sets the plotting origin. The default is 0.5,0.5. A null value in either field leaves the former value unchanged.

The following sets of control cards set up a disk file containing a loadable binary file and an UPDATE file. In each set the cards referring to disk files must be changed from application to application and the cards defining and/or saving the I/O file sets must be added.

I. Debug Initialization

This set of cards reads in the Fortran or compass cards using UPDATE. An UPDATE file is created and the decks are compiled. If either causes an error the run is aborted. If compilation is successful, a binary file is created. These files are combined and put in a permanent disk file with the binary as the first file. An execution is then attempted.

```
-JOB CARD-
COMMENT. DEBUG (AFGL/NOS) - INITIALIZATION
UPDATE(N,W,)
FTN (I=COMPILE, SL, T, R =3)
REWIND (LGO)
REQUEST (NL,*PF)
COPYBF(LGO,NL)
COPYBF(NEWPL,NL)
CATALOG(NL,MGOVLX,ID=
ATTACH (PLTLIB,TEKLIB)
ATTACH (HTWLlib, ID=
LIBRARY(HTWLlib,PLTLIB)
MAP(FULL)
LGO.
7/8/9
        UPDATE creation deck
7/8/9
        Program test data
7/8/9
6/7/8/9
```

II. Debug Testing

This set of cards compiles changes to UPDATE file and substitutes them using COPYL. This is for testing only and does not modify the disk file.

```
-JOB CARD-
COMMENT, DEBUG (AFGL/NOS) - TESTING
ATTACH (OL,MGOVLX, ID= )
COPYBF(OL,BIN)
UPDATE (P=OL,R=C,Q)
FTN (I=COMPILE, SL, T, OPT=0,R=3)
REWIND(BIN,LGO)
COPY(BIN,LGO,B)
ATTACH(PLTLIB,TEKLIB)
ATTACH(HTWLIB, ID= )
LIBRARY(HTWLIB,PLTLIB)
B.
7/8/9
    UPDATE Modification deck
7/8/9
    Program test data.
```

III. Debug Update

This set of cards modifies the UPDATE FILE and compiles a new binary file. After cataloging the new disk file a run is attempted.

```
-JOB CARD-
COMMENT, DEBUG (AFGL/NOS - UPDATE
ATTACH (OL,MGOVLX ID= )
SKIPF(OL,1,17)
UPDATE (N,P=OL,R=CN,W,F)
FTN(I=COMPILE,SL,T,R=3)
REWIND(LGO)
REQUEST(NL,*PF)
COPYBF(LGO,NL)
COPYBF(NEWPL,NL)
CATALOG(NL,MGOVLX, ID= )
ATTACH(PLTLIB,TEKLIB)
ATTACH(HTWLIB, ID= )
LIBRARY(HTWLIB,PLTLIB)
MAP(FULL)
LGO.
7/8/9
    UPDATE modification deck. (continued on next page)
```

7/8/9
Program test deck
7/8/9
5/7/8/9

IV. Production Run

This set of cards directly loads the program.

-JOB CARD-
ATTACH(OL,MGOVLX, ID=)
ATTACH(PLTLIB, TEKLIB)
ATTACH(HTWLIB, ID=)
LIBRARY(HTWLIB, PLTLIB)
OL.
7/8/9
Data Deck
7/8/9
6/7/8/9

V. Debug Audit

These control cardw ill list the binary decks in the binary file and the decks in the UPDATE FILE and will compile all decks to produce a listing. The list of binary decks includes the date of compilation, entry-point, and subroutines of each routine.

-JOB CARD-
COMMENT, DEBUG (AFGL/NOS) - AUDIT
ATTACH(OL,MGOVLX, ID=)
DISPOSE(OUTPUT,*PR=C)
SKIPF(OL,1,17)
UPDATE(P=OL,R=C,F,L=F)
FIN(I=COMPILE,SL,T,R=3)
REWIND(OL)
ATTACH(PLTLIB, TEKLIB)
ATTACH(HTWLIB, ID =)
LIBRARY(HTWLIB, PLTLIB)
MAP(FULL)
LOAD(OL)
NOGO.
6/7/8/9

SOME PROPERTIES OF SOLUTIONS OF THE PHOTOELECTRON FLUX EQUATIONS

The solution of

$$-ay''(x) - by'(x_0 + cy(x)) - dy(x+\Delta) = S(x)$$

on $[0, \infty)$ which

- 1.) is bounded on $[0, \infty)$,
- 2.) is continuous on $[0, \infty)$, and
- 3.) has continuous first derivative $y'(x)$ on $(0, \infty)$ with the property that $\lim_{x \rightarrow 0} y'(x)$ exists.

$$x \rightarrow 0$$

Let $S = u + iv$ be a complex variable and let

$$K(S) = S^2 - q + Pe^{\Delta S}$$

with

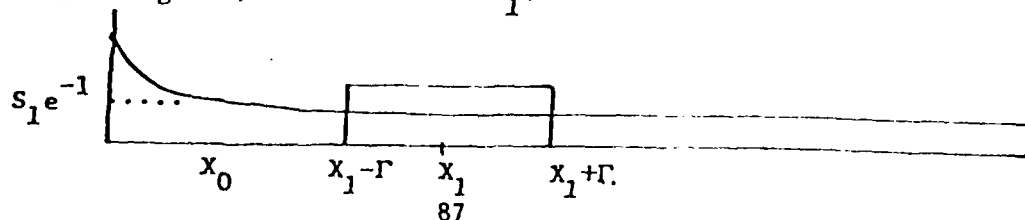
$$q = \frac{4ac+b^2}{4a^2} \quad \text{and} \quad P = \frac{d}{a} e^{-\frac{b}{2a}\Delta}$$

There can be at most one real zero of $K(S)$ which, if it occurs, must occur at $S_0 = \frac{1}{\Delta} - \sqrt{\frac{1}{\Delta^2} + q}$. This zero may be of order 1 or order 2. All other zeros of $K(S)$ are of order 1 and occur in conjugate pairs. Let $U_k \pm iv_k$ for $k = 1, \dots, n$ be all the zeros of $K(S)$ to the left of the line $\operatorname{Re}(s) = b/2a$ and $U_k \pm iv_k$ for $k = n+1, \dots$ be the zeros of $K(S)$ to the right of $\operatorname{Re}(s) = b/2a$.

(There are a countably infinite number of these).

CASE I. $S(x) = S_0 e^{-x/x_0} + S_1 r(x)$ where $r(x)$ is a rectangular pulse of

width 2Γ and height $1/2\Gamma$ centered at x_1 .



Let

$$H(x) = \frac{1}{(1/x_0^2 - q + p e^{-\Delta/x_0})} e^{-x/x_0} + (Ax+B) e^{(\frac{1}{\Delta} - \frac{b}{2a})x} -$$

$$\Delta^{1/2} + q) x + \sum_{k=1}^m A_k e^{(u_k - \frac{b}{2a})x} \cos(v_k x + \phi_k).$$

1A. For $x > x_1 + \Gamma$,

$$Y(x) = H(x) + \sum_{k=1}^m B_k e^{(u_k - \frac{b}{2a})(x - (x_1 + \Gamma))} \cos(v_k x + \psi_k)$$

$$+ C_k e^{(u_k - \frac{b}{2a})(x - (x_1 + \Gamma))} \cos(v_k x + \Psi_k)$$

1B. For $x_1 - \Gamma < x < x_1 + \Gamma$,

$$Y(x) = H(x) + \sum_{k=1}^m B_k e^{(u_k - \frac{b}{2a})(x - (x_1 - \Gamma))} \cos(v_k x + \psi_k)$$

$$+ \sum_{k=n+1}^m C_k e^{(u_k - \frac{b}{2a})(x - (x_1 + \Gamma))} \cos(v_k x + \theta_k)$$

1C. For $0 < x < x_1 - \Gamma$,

$$Y(x) = H(x) + \sum_{h=n+1}^m B_h e^{(u_h - \frac{b}{2a})(x - (x_1 + \Gamma))} \cos(v_h x + \psi_h)$$

$$+ C_k e^{(u_k - \frac{b}{2a})(x - (x_1 + \Gamma))} \cos(v_k x + \theta_k).$$

If s_0 is not a zero of $K(s)$ then $A=B=0$

If s_0 is a zero of $K(s)$ of order one then $A=0$ but B is arbitrary.

If s_0 is a zero of $K(s)$ of order two then A and B are both arbitrary.

2A. For $x > x_1$,

$$Y(x) = H(x) + \sum_{k=1}^n B_k e^{(u_k - \frac{b}{2a})(x-x_1)} \cos(v_k x + \psi_k)$$

2B. For $0 < x < x_1$,

$$Y(x) = H(x) + \sum_{k=m+1}^n B_k e^{(u_k - \frac{b}{2a})(x-x_1)} \cos(v_k x + \psi_k)$$

All the remarks about the constants, location of zeros of $K(s)$, etc. that followed Case I also can be applied to this case.

- DETAILS -

The solution of

$$-ay''(x) - by'(x_0 + cy(x)) - dy(x+\Delta) = S(x)$$

on $[0, \infty)$ which

- 1.) is bounded on $[0, \infty)$,
- 2.) is continuous on $[0, \infty)$, and
- 3.) has continuous first derivative $y'(x)$ on $(0, \infty)$ such that $\lim_{x \rightarrow 0} y'(x)$ exists

$$x \rightarrow 0$$

$$y''(x) + \frac{b}{a} y(x) - \frac{c}{a} y(x) + \frac{d}{a} y(x-\Delta) = -\frac{1}{a} S(x)$$

Change the dependent variable from y to z via the relation

$$y = z(x) e^{-\frac{b}{a}x}$$

This yields the equation

$$(4) z''(x_0 - q z(x) + p z(x+\Delta) = S^*(x)$$

where

$$q = \frac{4ac - b^2}{4a^2} \quad 0, \quad p = \frac{d}{2} e^{-\frac{b}{2a}\Delta} \quad 0, \quad S^*(x) = -\frac{1}{a} e^{\frac{b}{2a}x} S(x)$$

If $y(x)$ has properties 1, 2, and 3 listed above then $Z(xy)$ is $\sigma(e^{\frac{b}{2d}x})$ and has properties 2 and 3. Conversely, if $Z(x)$ is $\sigma(e^{\frac{b}{2a}x})$ and has properties 2 and 3 then $Y(x)$ has properties 1, 2, and 3.

If $Z_1(x)$ is a solution of the homogenous equation
 $(*) Z''(x) - aZ(x) + pZ(x+\Delta) = 0$

which is $\sigma(e^{\frac{b}{2a}x})$ and has properties 2 and 3 and $Z_2(x)$ is a solution of # with the same properties, then $Z_1(x) + Z_2(x)$ is also a solution of # with these same properties.

If we assume that $Z(x)$ is a solution of the homogenous equation * which is $0(e^{\frac{b}{2a}x})$ and has properties 2 and 3, then the Laplace transform

$$Z(s) = \int_0^\infty Z(x) e^{-sx} dx$$

converges on $\text{Re}(s) \geq \frac{b}{2a}$ and transforming all of * yields

$$Z(s) = \frac{z^1(0)}{K(s)} \frac{s + z(0)}{K(s)} + \frac{e^{s\Delta}}{K(s)} \int_0^\Delta z(t) e^{-st} dt$$

where $K(s) = s^2 - q + pe^{s\Delta}$.

The zeros of $K(s)$.

Setting $s = u + iv$ in $s^2 - q + pe^{s\Delta} = 0$, separating the real and imaginary parts and setting them equal to zero, and doing a little more algebra one finds that the zeros of $K(s)$ are in the intersection of the curves

$$u = v \cot \Delta v \pm \sqrt{v^2 \cot \Delta v + v^2 + q}$$

and

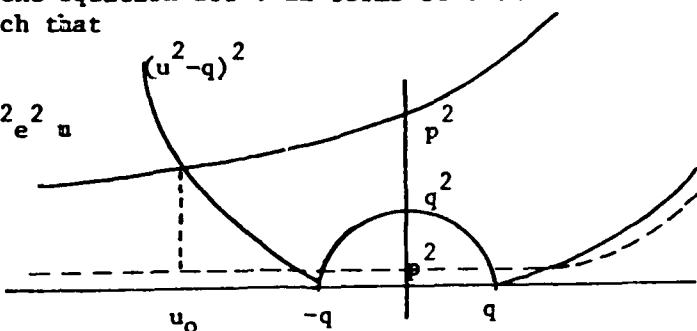
$$v = \sqrt{\sqrt{p^2 e^{2\Delta u} + 4q u^2} - (u^2 + q)}$$

Since v must be real, the equation for v in terms of u as defined only for those values of u such that

$$\sqrt{p^2 e^{2u} + 4q u^2} > u^2 + q > p^2 e^{2u}$$

or

$$p^2 e^{2u} \geq (u^2 - q)^2.$$



The curves of u and v are plotted for a sufficiently large value of p . The curves are symmetric w.r.t. the u axis so the lower halves have not been plotted.

$$K'(s) = 2s + p\Delta e^{\Delta s}$$

$$K''(s_0) = 2 + p\Delta^2 e^{s_0 \Delta}$$

$$K(s) = K'(s) = 0 \text{ implies that } s = \frac{1}{\Delta} \pm \sqrt{\frac{1}{\Delta^2} + q}$$

Therefore there is only one possible zero of order two of $K(s)$ at

$$s_0 = \frac{1}{\Delta^2} - \sqrt{\frac{1}{2} + q}$$

$K''(s_0) = 0$ implies that $v = \frac{\pi + n\pi}{\Delta}$ so there can be no zeros of order three or more.

All zeros of $K(s)$ are 1st order except perhaps a zero of order two at s_0 .

All zeros (except perhaps the zero at s_0) occur in conjugate pairs.

There are only a finite number of zeros to the left of $\operatorname{Re}(s) = \frac{b}{2a}$.

There are countably infinite number of zeros to the right of $\operatorname{Re}(s) = \frac{b}{2a}$.

If p is sufficiently small there will be no zeros of $K(s)$ to the left of $\operatorname{Re}(s) = \frac{b}{2a}$.

It is extremely unlikely that a zero of $K(s)$ lies on the line $\operatorname{Re}(s) = \frac{b}{2a}$ (probability zero), but it is possible.

If there are no zeros of $K(s)$ on $\operatorname{Re}(s) = \frac{b}{2a}$ one can use the Mellin inversion integral taken along the contour $\operatorname{Re}(s) = \frac{b}{2a}$ to find the solution of the homogeneous equation *.

$$Z(s) = \frac{1}{2\pi i} \int_{\frac{b}{2a} - i\infty}^{\frac{b}{2a} + i\infty} \frac{(Z(0) s + Z'(0)) e^{sx}}{K(s)} ds$$

$$+ \frac{1}{2\pi i} \int_{\frac{b}{2a} - i\infty}^{\frac{b}{2a} + i\infty} \left[\frac{e^{s\Delta}}{K(s)} \int_0^\Delta Z(t) e^{st} dt \right] e^{st} ds.$$

For $X > 0$ one may complete contours for the first integral using semi-circles in the half plane $\operatorname{Re}(s) \leq \frac{b}{2a}$ and use the Cauchy residue theorem to find that

$$\begin{aligned} \frac{1}{2\pi i} \int_{\frac{b}{2a} - i\infty}^{\frac{b}{2a} + i\infty} \frac{(Z(0) s + Z'(0)) e^{sx}}{s^2 - q + pe^{s\Delta}} ds &= (Ax+B)e^{\left(\frac{1}{\Delta} - \frac{1}{2a} - \frac{1}{\Delta^2} + q\right)} \\ &\quad + \sum_{k=1}^m a_k e^{s_k x} + \bar{a}_k e^{\bar{s}_k x} \\ &= (Ax+B)e^{\left(\frac{1}{\Delta} - \frac{b}{2a} - \sqrt{\frac{1}{\Delta^2} + q}\right)} \\ &\quad + \sum_{k=1}^{\infty} A_k e^{u_k x} \cos(v_k x + \phi_k) \end{aligned}$$

We now turn to the evaluation of

$$\frac{1}{2\pi i} \int_{\frac{b}{2a} - i\infty}^{\frac{b}{2a} + i\infty} \frac{e^{sx}}{K(s)} \left[\int_0^\Delta z(t) e^{-st} dt \right] e^{sx} ds$$

$\int_{\frac{b}{2a} - i\infty}^{\frac{b}{2a} + i\infty} \frac{e^{s(x-(\Delta-t))}}{K(s)} ds$ converges uniformly for $t \in [0, \Delta]$, hence

$$\int_0^\Delta dt z(t) \int_{\frac{b}{2a} - i\infty}^{\frac{b}{2a} + i\infty} \frac{e^{s(x+(\Delta-t))}}{K(s)} ds = \int_{\frac{b}{2a} - i\infty}^{\frac{b}{2a} + i\infty} \frac{e^s}{K(s)} \left[\int_0^\Delta z(t) e^{-st} dt \right] e^{sx} dx.$$

(and $\Delta - t \geq 0$ for $t \in [0, \Delta]$)

so as long as $x \geq 0$ one may again complete contours using semi-circles in the half plane $\operatorname{Re}(s) \leq \frac{b}{2a}$ and the Cauchy residue theorem to find that

$$\frac{1}{2\pi i} \int_{\frac{b}{2a} - i\infty}^{\frac{b}{2a} + i\infty} \frac{e^{s(x + (\Delta-t))}}{K(s)} = (Ax + B) e^{s\Delta(x + (\Delta-t))} + \sum_{k=1}^M b_k e^{s_k(x + (\Delta-t))} \bar{s}_k(x + b_k e)$$

and

$$\begin{aligned}
 & \frac{1}{2\pi i} \int_0^{\Delta} dt Z(t) \int_{\frac{b}{2a} - i\infty}^{\frac{b}{2a} + i\infty} \frac{e^{S(x+(\Delta-t))}}{K(s)} ds = (A' x + B') e^{S_0 X} \\
 & + \sum_{k=1}^m b'_k e^{S_k X} + b'_k e^{\bar{S}_k \lambda} \\
 & = (A' x + B') e^{S_0 X} + \sum_{k=1}^m B_k e^{u_k \lambda} \\
 & \cos(v_k \lambda + \Psi_k)
 \end{aligned}$$

Since it is easily verified that $e^{S_k X}$ is a solution of the homogenous equation * if and only if S_k is a zero of $K(s)$, and in case S_0 is a zero of order 2 than $e^{S_0 X}$ is a solution of *, it follows that the constraints A , B , A_k , A' , B' , and B_k in the above evaluation of the two integrals are all arbitrary. We may combine the results of both integrations to find that the general solution of * which is $\Theta(e^{\frac{b}{2a} X})$ and satisfied properties 2 and 3 is,

$$(Ax + B) e^{S_0 X} + \sum_{k=1}^n A_k e^{u_k X} \cos(v_k + \Phi_k)$$

$S_k = u_k + i v_k$ and \bar{S}_k are the zeros to the left of $\text{Re}(s) = \frac{b}{2a}$ except for possibly a zero at S_0 . If S_0 is not a zero of $K(s)$ then $A=B=0$. If S_0 is a zero of order 1, then $A=0$.

If one now assumes that $Z(x)$ is a solution of the non-homogeneous equation * which is $\Theta(e^{\frac{b}{2a} X})$ and satisfies 2 and 3, then taking the Laplace transform of # and inverting leads to;

$$Z(x) = \frac{1}{2\pi i} \int_{\frac{b}{2a} - i\infty}^{\frac{b}{2a} + i\infty} \frac{(Z(s) s + Z'(s)) e^{sx}}{K(s)} + \frac{1}{2\pi i} \int_{\frac{b}{2a} - i\infty}^{\frac{b}{2a} + i\infty} \frac{e^s}{K(s)} \left[\int_0^\Delta z(t) e^{-st} dt \right] e^{sx}$$

$$+ \frac{1}{2\pi i} \int_{\frac{b}{2a} - i\infty}^{\frac{b}{2a} + i\infty} \frac{s_+^*(s) e^{sk}}{K(s)} ds, \text{ where } s_+^*(s) = \mathcal{J}\{s^*(x)\}.$$

Even though $Z(x)$ is now a solution to the non-homogeneous equation # rather than the homogeneous equation *, the evaluation of the first two integrals proceeds in exactly the same way as in the homogeneous case and gives only solutions to the homogeneous equation *. Therefore, the most general solution of

$$Z''(x) - q Z(x) + p Z(x+\Delta) = S^*(x)$$

of $\sigma(e^{\frac{a}{2b}x})$ which satisfied properties 2 and 3, provided it exists, is given by

$$Z(x) = (Ax+B)e^{S_0 x} + \sum_{k=1}^m A_k e^{u_k x} \cos(v_k x + \Phi_k) + \frac{1}{2i} \int_{\frac{b}{2a} - i\infty}^{\frac{b}{2a} + i\infty} \frac{s_+^*(s)}{K(s)} e^{sx} ds.$$

One can now check $Z(x)$ and find that it does satisfy # and is of $\mathcal{O}(e^{-\frac{a}{2b}X})$, and satisfied properties 2 and 3.

The results for Case I and Case II are obtained by evaluating the last integral in the expression for $Z(x)$ and multiplying $Z(x)$ by $e^{-\frac{b}{2b}X}$. Keep in mind that for certain values of X contours must be completed in the half plane $\text{Re}(s) \leq \frac{b}{2a}$ while for other values of X the contours must be completed in the half plane $(\text{Re}(s) \geq \frac{b}{2a})$. This last procedure leads to the sum of an infinite number of terms because there are an infinite number of roots of $K(s)$ in the right half plane.

Solutions to special cases of

$$(1) \quad C(x)Z(x) = S(x) + \int_{x+\Delta}^{\infty} K(r,x) Z(r) dr.$$

In the paper "Degradation and High Energy Scattering of Radiation" V. Fano solves certain equations of the type

$$\mu(E) n(E) = \int_0^{\infty} (E+r, r) n(E+r) dr + S(E)$$

by observing that when $S(E)$ is the unit impulse function $S(E-E_0)$ the equation can, under certain restrictions on the kernel, be converted to an equation in which the integral is a convolution integral. This makes the resulting equation amenable to transform techniques. If $S(x)$ is the unit impulse function equation (1) can also be converted to an integral equation in which, again under certain conditions, the integral can be written as a convolution integral. The resulting equation still contains a term with an advanced argument, but in many cases this equation can also be solved using Laplace transforms.

First, assume that $c(x) > 0$ on $[0, \infty)$ and let $y(x) = c(x)Z(x)$ and $k(r,x) = K(r,x)/C(r)$. Then

$$(1A) \quad Y(x) = S(x) + \int_{x+\Delta}^{\infty} k(r,x) y(r) dr$$

AD-A102 346

BEDFORD RESEARCH ASSOCIATES MA
DEVELOPMENT OF MATHEMATICAL MODELS IN SUPPORT OF AFGL ATMOSPHER--ETC(U)
MAY 80 T M COSTELLO, J P NOONAN F19628-78-C-0083

F/G 4/2

NL

UNCLASSIFIED

AFGL-TR-80-0296

2 of 2
40 A
02440

END
DATE
FILED
8-81
DTIC

Also assume that $S(x) = S(x - X_0)$ and that $X_0 > 2\Delta$. Define a function $u(x)$ in three parts as follows:

A. - on $0 \leq X \leq X_0 - 2\Delta$, $u(x)$ is a solution of the equation

$$u(x) = \int_{x+\Delta}^{X_0-\Delta} k(r, x) u(r) dr + k(X_0, x)$$

B. - on $X_0 - 2\Delta \leq X \leq X_0 - \Delta$, $u(x) = k(X_0, x)$

C. - on $X \geq X_0 - \Delta$, $u(x) = 0$

Now let $f(x) = u(x) + S(x - X_0)$. Then

$$\int_{x+\Delta}^{\infty} k(r, x) f(r) dr = \int_{x+\Delta}^{\infty} k(r, x) u(r) dr + \int_{x+\Delta}^{\infty} k(r, x) S(r - X_0) dr$$

$$= \left\{ \begin{array}{l} A. \quad 0 \leq X \leq X_0 - 2\Delta, \int_{x+\Delta}^{X_0-\Delta} k(r, x) u(r) dr + k(X_0, x) = u(x) \\ B. \quad X_0 - 2\Delta \leq X \leq X_0 - \Delta, \quad k(X_0, x) = u(x) \\ C. \quad X \geq X_0 - \Delta, \quad 0 = u(x) \end{array} \right.$$

Thus,

$$\int_{x+\Delta}^{\infty} k(r, x) f(r) dr + S(x - X_0) = u(x) + S(x - X_0) = f(x)$$

Therefore, what one really needs to solve (1A) in this case ($S(x) = S(x-x_0)$) is the solution of the integral equation

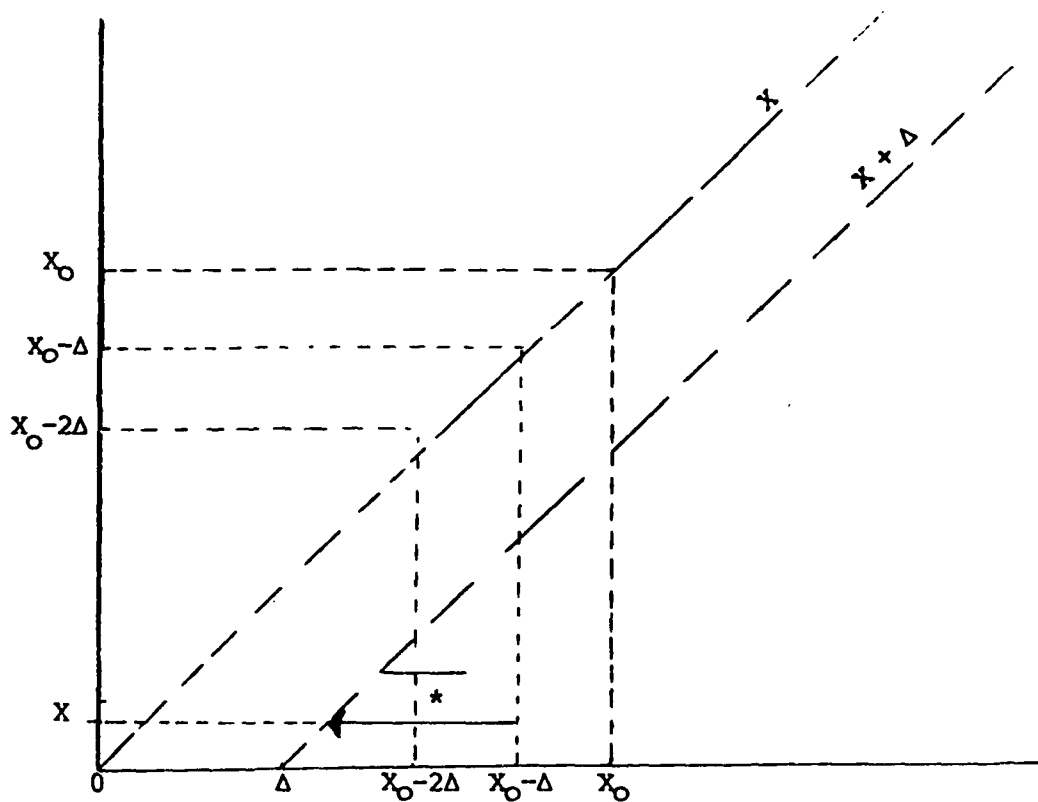
$$(2) \quad U(x) = \int_{x-\Delta}^{x_0 - \Delta} k(r, x) u(r) dr + k(x_0, x)$$

on the interval $0 \leq x \leq x_0 - 2\Delta$. However, note that r varies up to $x_0 - \Delta$ in the above integral so that the values of $u(r)$ up to $x_0 - \Delta$ enter into equation (2).

To cast equation (2) in a different form, first change the variable of integration by letting $s = x_0 - \Delta - r$. Then $r = x_0 - \Delta - s$ and $0 \leq s \leq x_0 - 2\Delta - x$. Equation (2) becomes

$$(3) \quad u(x) = \int_0^{x_0 - x - 2\Delta} k(x_0 - \Delta - s, x) u(x_0 - \Delta - s) ds + K(x_0, x)$$

observe that $x_0 - \Delta - s$ varies from $x_0 - \Delta$ to $x + \Delta$.



Now change the independent variable by letting $t = X_0 - x - 2\Delta$. Then $x = X_0 - 2\Delta - t$ and, since $0 \leq x \leq X_0 - 2\Delta$ we find that $0 \leq t \leq X_0 - 2\Delta$.
 Equation (3) now becomes

$$(4) \quad u(X_0 - 2\Delta - t) = \int_0^t k(X_0 - \Delta - s, X_0 - 2\Delta - t) u(X_0 - \Delta - s) ds + k(X_0, X_0 - 2\Delta - t)$$

Note that even though $X_0 - 2\Delta - t$ varies from 0 to $X_0 - 2\Delta$, $X_0 - \Delta - t$ varies up to $X_0 - \Delta$.

Now change the unknown function from u to v by letting
 $u(t) = v(X_0 - \Delta - t)$. Equation (4) becomes

$$(5) \quad v(t+s) = \int_0^t k(X_0 - \Delta - s, X_0 - 2 - t)(s) ds + k(X_0, X_0 - 2\Delta - t)$$

That is, if one can find a solution of (5) for $0 \leq t \leq X_0 - 2\Delta$ (which means also that $\Delta \leq t + \Delta \leq X_0 - \Delta$) then by letting $u(t) = v(X_0 - \Delta - t)$ we find that $u(f)$ satisfies equation (4).

Initially, one is interested in functions $v(t)$ defined on $[0, X_0 - \Delta]$ which satisfy (5.) for t in $[0, X_0 - 2\Delta]$. One could try to solve (5.) by generalizing standard integral techniques (Neumann series). This possibility will be investigated later. Instead, we assume that

$$k(X_0 - \Delta - , X_0 - 2\Delta - t) = g(t-s)$$

over the region $t \geq 0$ and $0 \leq s \leq t$, and that the Laplace transform of $g(x)$ exists. An example of such a kernel will be given later. Under the assumption, equation (5) becomes

$$(6) \quad v(t + \Delta) = \int_0^t g(t-s)v(s) ds + g(t+\Delta)$$

We look for solutions to (6) over $[0, \infty)$. These will also be solutions over $[0, X_0 - \Delta]$. (It is also possible to look for solutions to (6) on $[0, X_0 - \Delta]$ using finite Fourier transforms and trying to work out a convolution integral theory for such transforms. This possibility will also be investigated later).

One should not forget that on $[X_0 - 2, X_0 - \Delta]$ we must have $u(t) = K(X_0, t)$. Therefore, for $0 \leq t \leq \Delta$,

$$(7) \quad v(t) = u(X_0 - \Delta - t) = R(X_0, -\Delta - t) = g(t)$$

Now take the Laplace transform of equation (6.)

$$\int_0^\infty v(t + \Delta) e^{-pt} dt = G(p) V(p) + \int_0^\infty g(t + \Delta) e^{-pt} dt$$

Let $W = t + \Delta$. Then we have (Here $G(p)$ and $V(p)$ are the transforms of $g(x)$ and (x) , respectively.

$$\begin{aligned} \int_\Delta^\infty v(w) e^{-p(w-s)} dw &= G(p) V(p) + \int_\Delta^\infty g(w) e^{-p(w-\Delta)} dw \\ e^{p\Delta} \left\{ \int_0^\infty v(w) e^{-pw} dw - \int_0^s v(w) e^{-pw} dw \right\} &= \\ G(p) V(p) - e^{p\Delta} \left\{ \int_0^\infty g(w) e^{-pw} dw - \int_0^\Delta g(w) e^{-pw} dw \right\} & \end{aligned}$$

$$e^p V(p) = G(p) V(p) + e^{p\Delta} G(p)$$

$$V(p) \left\{ e^{p\Delta} - G(p) \right\} = e^{p\Delta} G(p)$$

$$V(p) = \frac{e^{p\Delta} G(p)}{e^{p\Delta} - G(p)}$$

It can be shown that the zeros of $e^{p\Delta} - G(p)$ lie in a half plane $\text{Re } p \leq a$ for a sufficiently large. If one can also find an a such that the integral in

$$(8) \quad v(t) = \frac{1}{2\pi i} \int_{a-i\infty}^{a+i\infty} \frac{e^{p\Delta} G(p)}{e^{p\Delta} - G(p)} e^{pt} dp$$

converges uniformly for $t > 0$ and $\frac{e^{p\Delta} G(p)}{e^{p\Delta} - G(p)}$ is of order $0(|p|^R)$ for some $k > 0$, then (8.) defines a function on $[0, \infty)$ which satisfies both equation (6.) and boundary (7.).

To show the function defined in *8) satisfies equation (6), we proceed as follows:

$$\int_0^t g(t-s) (s) ds = \frac{1}{2\pi i} \int_{a-i\infty}^{a+i\infty} dp \frac{e^{p\Delta} G(p)}{e^{p\Delta} - G(p)} \int_0^t g(t-s) e^{ps} ds$$

$$= \frac{1}{2\pi i} \int_{a-i\infty}^{a+i\infty} \frac{e^{p\Delta} G(p)}{e^{p\Delta} - G(p)} e^{pt} \int_0^{a-t} g(d) e^{-pd} da$$

$$= \frac{1}{2\pi i} \int_{a-i\infty}^{a+i\infty} \frac{e^p G(p)}{e^p - G(p)} e^{pt} \left\{ G(p) - \int_t^\infty g(\alpha) e^{-p\alpha} d\alpha \right\}$$

$$= \frac{1}{2\pi i} \int_{a-i\infty}^{a+i\infty} \frac{e^{p\Delta} G(p)^2 e^{pt}}{e^{p\Delta} - G(p)} dp - \int_0^t g(\alpha) d\alpha \frac{1}{2\pi i}$$

$$\int_{a-i\infty}^{a+i\infty} \frac{e^{p\Delta} G(p)}{e^{p\Delta} - G(p)} P(t\alpha) dp$$

If $\frac{e^{p\Delta} G(p)}{e^{p\Delta} - G(p)}$ is $0 (|p|^k)$ for some $R > 0$ then the contour in the

last integral in the above equation can be completed to the right. Since $e^{p\Delta} - G(p)$ has no zeros in this half plane

$$\frac{1}{2\pi i} \int_{a-i\infty}^{a+i\infty} \frac{e^{p\Delta} G(p)}{e^{p\Delta} - G(p)} e^{-p(t-\alpha)} dp = 0 \text{ if } t - \alpha < 0$$

Thus,

$$\int_0^t g(t-s) v(s) ds - \frac{1}{2\pi i} e^{p\Delta} G(p) \left(\frac{G(p)}{e^{p\Delta} - G(p)} \right) e^{pt} dp =$$

$$\frac{1}{2\pi i} \int_{a-i\infty}^{a+i\infty} e^{p\Delta} G(p) \left[\frac{e^{p\Delta}}{e^{p\Delta} - G(p)} - 1 \right] e^{pt} dp =$$

$$\frac{1}{2\pi i} \int_{a-i\infty}^{a+i\infty} \frac{e^{p\Delta} G(p) e^{p(t+\Delta)}}{e^{p\Delta} - G(p)} dp - \frac{1}{2\pi i} \int_{a-i}^{a+i} G(p) e^{p(t+\Delta)} dp$$

$$= \gamma(t + \Delta) - g(t + \Delta)$$

$$\text{Hence, } v(t + \Delta) = \int_0^t g(t-s) v(s) ds + g(t+\Delta)$$

To show that $v(t) = g(t)$ for $0 \leq t \leq s$, observe that

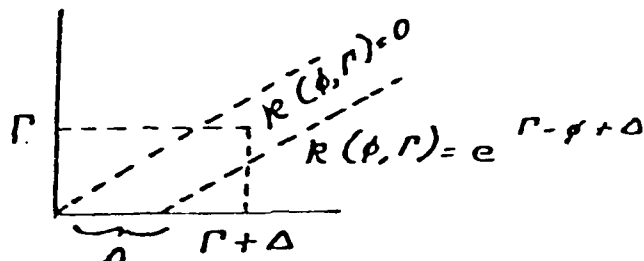
$$\begin{aligned}
 v(t) &= \frac{1}{2\pi i} \int_{a-i\infty}^{a+i\infty} \frac{e^{p\Delta} G(p)}{e^{p\Delta} - G(p)} e^{pt} dp = \\
 &\quad \frac{1}{2\pi i} \int_{a-i\infty}^{a+i\infty} \left(G(p) + \frac{G(p)^2}{e^{p\Delta} - G(p)} \right) e^{pt} dp \\
 &= \frac{1}{2\pi i} \int_{a-i\infty}^{a-i\infty} G(p) e^{pt} dp + \frac{1}{2\pi i} \int_{a-i\infty}^{a+i\infty} \frac{G(p)^2}{p\Delta - G(p)} e^{pt} dp = \\
 g(t) &+ \frac{1}{2\pi i} \int_{a-i\infty}^{a+i\infty} \frac{G(p)^2 e^{p(t-\Delta)}}{1 - e^{-p\Delta} G(p)} dp \\
 \text{But } & \frac{1}{2\pi i} \int_{a-i\infty}^{a+i\infty} \frac{G(p)^2 e^{p(t-\Delta)}}{1 - e^{-p\Delta} G(p)} dp = 0 \text{ if } 0 \leq t \leq \Delta \text{ because in}
 \end{aligned}$$

this case the contour may be completed in the right half plane $\operatorname{Re} p > 0$ and $1 - e^{-p\Delta} G(p)$ has no zeros there (and $G(p)$ is analytic there).

$$f(x) = \begin{cases} \frac{1}{2\pi i} \int_{a-i}^{a+i} \frac{G(p) e^{px_0 - pt}}{d p^\Delta - G(p)} dp & \text{on } [0, x_0 - \Delta] \\ \delta(x - x_0) & \text{otherwise} \end{cases}$$

An Example

$$\text{Let } k(\theta, s) = \begin{cases} e^{\Gamma - \theta + \Delta} & \text{for } \theta > \Gamma + \Delta \\ 0 & \text{otherwise} \end{cases}$$



Then $k(x_0 - \Delta - s, x_0 - 2\Delta - t) = e^{-(t-s)}$ for $t - \Delta > 0$.

and $k(x_0 - \Delta - s, x_0 - 2\Delta - t) = 0$ for $t - s < 0$.

$$\text{Therefore, let } g(x) = \begin{cases} e^{-x} & \text{for } x > 0 \\ 0 & \text{otherwise} \end{cases}$$

Then $(x_0 - \Delta - s, x_0 - 2s - t) = g(t-s)$ and g has a Laplace transform.

$$G(p) = \int_0^\infty e^{-(p+1)r} dr = \frac{1}{p+1} \text{ provided } \operatorname{Re} p > -1$$

$$g(t) = \frac{1}{2\pi i} \int_{a-i}^{a+i} \frac{e^{pt}}{p+1} dp \text{ provided } \operatorname{Re} a > -1$$

$$g(t) = \frac{1}{2\pi i} \int_{a-1}^{a+1} \frac{e^{pt}}{p+1} dp \quad \text{provided } \operatorname{Re} a > -1$$

$$(9) \quad v(t) = \frac{1}{2\pi i} \int_{a-1}^{a+1} \frac{e^{p(t+\Delta)}}{(p+1)e^{p\Delta-1}} dp$$

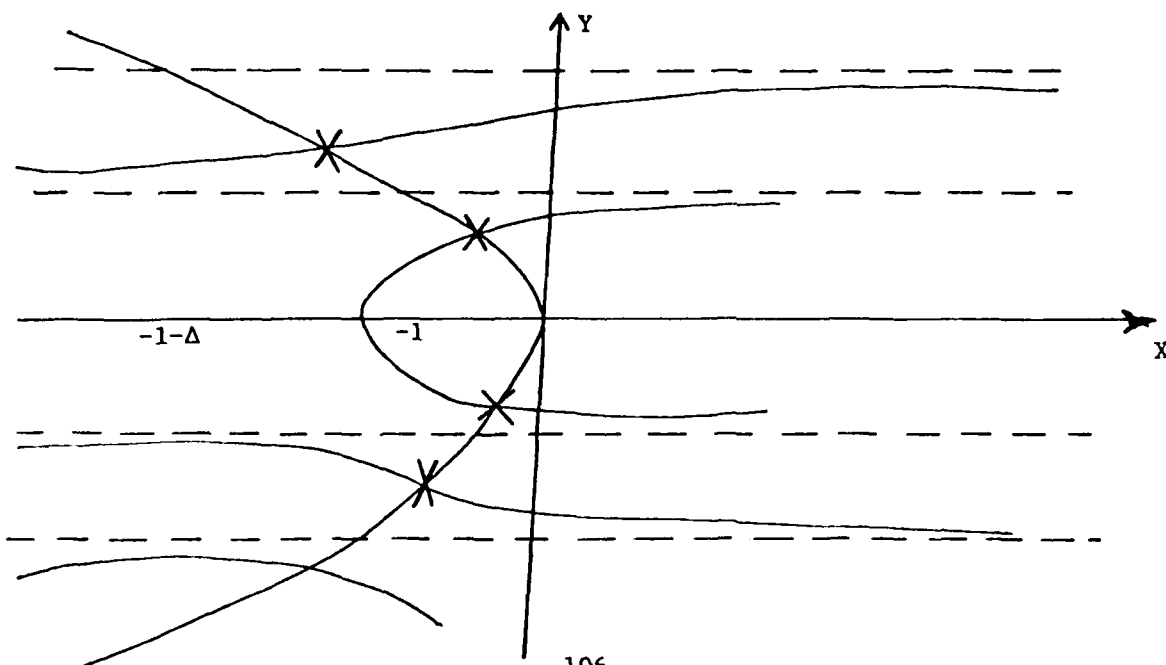
The zeros of $(p+1)e^{p\Delta-1}$ are located on the intersection of the curves

$$x = -(1+y \cot y s)$$

and

$$y^2 = e^{-2} - (x+1)^2$$

and all lie to the left of the imaginary axis. They also occur in conjugate pairs.



Thus, in the integral in (9.) we take a so that $Z_0 < a < 0$ where Z_0 is the real part of the first zeros to the left of the imaginary axis.

$$H(p) = \frac{e^p}{(p+1) e^{p\Delta} - 1} \text{ is of } O(|p|^{-1})$$

as $p \rightarrow \infty$ in the half plane $\operatorname{Re} p > a$ and $H(p)$ is analytic there so $v(t)$ defined in (9) is a solution of (6) in this special case provided the integral in (9) converges uniformly. Since $H(p)$ is $O(|p|^{-1})$ as $p \rightarrow \infty$ in the left half plane also, we can complete the contour of the integral in (9) in the left half plane also and find that (assuming all poles are of order 1)

$$v(t) = \sum_{i=1}^{\infty} \frac{e^{pi\Delta}}{\Delta(p_i + 1)} e^{pit} - p_i e^{pi\Delta}$$

$$= \sum_{i=1}^{\infty} \frac{e^{pit}}{\Delta - p_i}$$

where $\{p_i\}_{i=1}^{\infty}$ are all the roots of $(p+1) e^{p\Delta} - 1 = 0$.

Summing by pairing the complex conjugates, we find that

$$v(t) = \sum_{i=1}^N \frac{2e^{xit} \left[(\Delta - x_i) \cos y_i t + y_i \sin y_i t \right]}{(\Delta - x_i)^2 + y_i^2}$$

where $p_i = x_i + iy_i$. This last series is uniformly convergent for $t \geq 0$, so (9) is also uniformly convergent to $t \geq 0$.

In this special case, the solution to (1 Δ) is

$$f(x) = \begin{cases} \frac{1}{2\pi i} \int_{a-i}^{a+i} \frac{e^{-pt} (x_0 - t)}{(p+1) e^{p\Delta} - 1} dp & \text{on } [0, x_0 - \Delta] \\ 0 & \text{otherwise} \end{cases}$$

ANGULAR BEHAVIOR OF PHOTOPRODUCTION

The upper atmosphere has many effects of interest, among them are refraction and attenuation of radio waves, absorption of ultraviolet radiation, and the slowing of low satellites. The behavior of the upper atmosphere is controlled by the sun through many links, primarily the ultraviolet radiation whose effect varies diurnally through the solar zenith angle. Other links which may be significant but which are harder to model are through solar particles which are funnelled by the earth's magnetic field and may be approximately diurnal, as the solar wind, or sporadic, as particle bursts from solar flares. A detailed model is needed to understand the relative importance of different causes and effects and to identify the limits of various approximations and empirical relations.

To model the upper atmosphere in detail is difficult because it varies with time and with position, distance above the earth. An even greater and more significant problem is the fact that the ionosphere is a plasma which requires the modification of the Boltzmann equation, the standard basic equation of kinetic theory, through the use of Fokker-Planck methods. Due to the nonlinearity of the resulting integro-differential equation no solutions are known except for very simple cases. Dr. Jasperse has approached this modelling problem by first modelling only the electron distribution function using as given a neutral model atmosphere, the solar radiation, and the exospheric temperature. The energy distribution of the atoms, molecules, and ions were assumed to be Maxwellian. The resulting nonlinear integro-differential equation had terms for photoionization, recombination, electron-neutral elastic collisions, excitation collisions, de-excitation collisions, impact ionization collisions, and collisions between charged particles. A stable iterative calculational method was found to solve the equation numerically. The program has been used to model the atmosphere measured by a rocket flight. Further checking is desirable. This work should be continued to identify the significant interactions and parameters in the present model.

With the understanding gained, further work would consider effects not included in the present model. One such is diffusion but its inclusion would require more detailed calculational modelling of the vertical structure of the atmosphere. The inclusion of diffusion and of modelling the density of the atmospheric constituents would allow one to study and possibly predict the effect of solar activity on radio communication and the slowing of satellites.

Let the initial state, I , with spin projection M be represented by $|IM\rangle$. Let $|F'M'\mu\rangle$ be the final state of the ion in State F' with spin projection M' and an electron with momentum \vec{p} and spin projection μ . The interaction with a photon of momentum \vec{k} and polarization $\hat{\epsilon}$ is

$$\sigma = \vec{A} \cdot \vec{p} + \frac{1}{2} \vec{gH} \cdot \vec{s}$$

where

$$\vec{A} = \hat{\epsilon} e^{i\vec{k} \cdot \vec{r}}$$

$$\vec{H} = \vec{\Delta} \times \vec{A} = i\vec{k} \hat{\eta} e^{i\vec{k} \cdot \vec{r}}$$

and

$$\hat{\eta} = \vec{k} \times \hat{\epsilon}.$$

The cross section is

$$d\sigma = \frac{1}{2I+1} \sum_M \sum_{M'\mu} d\sigma_{MM'\mu} \propto \frac{1}{2I+1} \sum_{MM} \left| \langle F'M', \vec{p} \mu | 0/IM \rangle \right|^2$$

Using the relations from Brink and Satchler's book "Angular Momentum" on page 151:

$$\delta^3(\vec{p}-\vec{p}') = \frac{1}{4\pi} p^2 \delta(p-p') \sum_{lm} c_m^l(p) c_m^l(p')^*$$

$$e^{i\vec{k} \cdot \vec{r}} = \sum_k (-i)^k (2k+1)^{3/2} J_k(kr) \left(C^k(k) C^k(Y) \right)^\circ$$

where

$$\left(C^k(k) C^k(r) \right)^o = \sum_{mm'} C_m^k(k) C_{m'}^k(r) \langle km km' / 0 0 \rangle.$$

The final state and the interaction operator can be expanded:

$$\langle F' M' p_\mu \rangle = \sum_{F\ell m} / F' M' p_\ell m \frac{1}{2} \mu ; FM \rangle A^{F\ell}(p) \hat{\sigma}_m^{\ell *} \quad (1)$$

$$\hat{\sigma} = \sum_k \left(\sigma_E^k \left(\hat{\epsilon}^{k-1} \hat{\epsilon} \right)^k \right)^o + \left(\sigma_M^k \left(\hat{\eta}^{k-1} \hat{\eta} \right)^k \right)^o \quad (2)$$

$$\text{where } \hat{\sigma}_m^{\ell} = \frac{2^\ell \ell! \ell!}{(2\ell)!} C_m^\ell(p) \quad (3)$$

is a symmetric traceless tensor formed from the vector \hat{p} and σ_E^k and σ_M^k are the properly normalized electric and magnetic $\frac{1}{2}^\ell$ pole operators.

Using the reduced matrix elements the sums over the projections can be carried out:

$$d\sigma = \sum \text{(factors}_1 \left(\hat{\sigma}_m^{\ell} \left(\hat{\pi}^{k-1} \hat{\pi} \right)^k \hat{\sigma}_m^{\ell'} \left(\hat{\pi}'^{k'-1} \hat{\pi}' \right)^{k'} \right)^o \quad (4)$$

where $\hat{\pi}$ and $\hat{\pi}'$ are $\hat{\epsilon}$ and/or $\hat{\eta}$. The summations can be rearranged via 6-j and 9-j symbols:

$$\begin{aligned} d\sigma &= \sum \text{(factors}_2 \left(\left(\hat{\sigma}_m^{\ell} \hat{\sigma}_m^{\ell'} \right)^{\bar{\ell}} \left(\left(\hat{\pi}^{k-1} \hat{\pi} \right)^k \left(\left(\hat{\pi}'^{k'-1} \hat{\pi}' \right)^{k'} \right)^{\bar{\ell}} \right)^o \right. \\ &\quad \left. = \sum \text{(factors}_3 \left(\hat{\sigma}_m^{\ell} \left(\left(\hat{\pi}^{k-1} \hat{\pi}^{k'-1} \right) \left(\hat{\pi} \hat{\pi}' \right)^{\bar{\ell}} \right)^o \right) \end{aligned} \quad (5)$$

Summing over the photon polarization directions

$$\Sigma(\hat{\pi} \hat{\pi}') \propto \hat{\pi}^{k-1} \hat{\pi}$$

since \hat{k} is the only remaining direction.

Thus

$$\begin{aligned} d\sigma &= \sum \text{(factors}_4) \left((p)^{\bar{\ell}} \left((k)^{\bar{k}} (\hat{k})^{\bar{n}} \right)^{\bar{\ell}} \right)_0 \\ &= \sum \text{(factors}_5) \left((p)^{\bar{\ell}} (k)^{\bar{k}} \right)^{\bar{\ell}}_0 \\ &= \sum \text{(factors)}_{\bar{\ell}} p_{\bar{\ell}} (\cos \Theta) \end{aligned}$$

where

$$\cos \Theta = \hat{p} \cdot \hat{k}$$

If the highest multiple considered is $2^{k_{\max}}$, since $\ell = k \text{ (x) } k'$,
 $\ell_{\max} = 2^{k_{\max}}$.

Parity is conserved and the states have well determined parity.
The non-zero operators must all have a definite parity. Therefore, all terms $(\hat{k}^{k-1} \hat{n})^k$ of interest must have the same parity and
 $\langle (\hat{k}^{k-1} \hat{n})^k ((\hat{k})^{k'-1} \hat{n}')^{k'} \rangle^{\bar{\ell}}$ must have positive parity. This is reduced to (k) which has parity $(-)^\ell$. Thus ℓ must be even. A detailed reduction leads to the same result.

ATMOSPHERIC TURBULENCE MODELLING IMPACTING
STRATOSPHERIC ENVIRONMENT PROGRAM

Efforts conducted under this research impact the stratosphere chemical--Transport Model Development. The objectives and relevance are stated as follows:

OBJECTIVES: Develop methods of describing the constituents and thermal distributions of the normal stratosphere and calculate how these distributions are affected by Air Force flight operations and atmospheric transport coefficients; characterize stratospheric disturbances that can be produced from mountain waves and underlying thunderstorm activity. Develop specialized numerical techniques to incorporate radiation transfer and couple photochemical processes with the heat balance of the stratosphere.

RELEVANCE: This task is the key to the stratospheric environment project wherein the results of the various measurements are used to establish a realistic model of the stratosphere. The model, in turn, is used to predict if environmental changes will occur as a result of AF flight operation. This task is essential to the preparation of environmental impact statements of the Air Force.

The major effort of this work here on turbulence modelling is to improve stratospheric models for the prediction of Air Force systems operations in the stratosphere. In particular, the probability of occurrence of turbulence for a given location and season as a function of altitude is a required input to the tropospheric/stratospheric model used to predict effects of Air Force Systems emission pollutants in the stratosphere. Thus we are investigating the seasonal variability of the characteristic layers of turbulence in the troposphere and stratosphere and determining the seasonal variations in the natural levels of NO_x trace constituents which are also engine combustion by-products. This will result in refinements in the troposphere/stratosphere 1-D and 3-D chemical/radiative transport models

which are used to predict environmental effects, such as ozone depletion, caused by Air Force Systems emissions in the troposphere and stratosphere.

Meteorological data (temperature, winds, pressure and relative humidity) in the height range 0-60 km on magnetic tape is currently being restructured to provide efficient, easy access for processing with minimum computer time. A statistical approach is being used to determine the seasonal probability of occurrence of turbulence as a function of latitude, longitude and altitude through the use of the Richardson criteria for the presence or absence of turbulence in the atmosphere. NO_x trace constituents measured by LKD will be compared with data from other experimental techniques to determine the extremes of seasonal variability in these constituents. The turbulence and NO_x seasonal results will be used to parameterize the important role of transport processes and provide fine adjustments in the trapospheric/stratospheric chemistry of the 1-D and 3-D models.

Introduction:

The stratospheric seasonal variations task under the Stratospheric Environment Project is currently studying the general aspects of turbulence in the troposphere and lower stratosphere. The data being used in this study has been provided by the Environmental Data Service National Climatic Center in Asheville, North Carolina. The "rawinsonde data" consists of winds, temperature and pressure as a function of altitude obtained from all available stations (currently 144 stations) for the period 1948-1976. At the present time only 1970-1976 data have been reformatted for processing on the CDC 6600 computer system. This data is being used in calculating the Richardson number, a stability criteria for determining the presence or absence of atmospheric turbulence, and is given by the following relationship:

$$R_1 = g/T \left[\frac{\partial T}{\partial z} + \Gamma \right] / \left[\frac{\partial U}{\partial z} \right]^2$$

where: g is the acceleration of gravity

$\frac{\partial T}{\partial z}$ is the vertical temperature gradient

Γ is the dry adiabatic lapse rate (10^0 K/km)

and $\left[\frac{\partial U}{\partial z} \right]^2 = \left[\left(\frac{\partial v_x}{\partial z} \right)^2 + \left(\frac{\partial v_y}{\partial z} \right)^2 \right]$ is the square

of the vertical shear of the horizontal winds.

The rawinsonde system is not ideally suited to take measurements to provide thermodynamic data at the required sampling intervals for this application. The data being used in this study was intended to provide northern hemisphere pressure maps for a number of milibar pressure levels. In order to determine the Richardson number at equal height intervals, the temperature and wind component data points are fit using a Hermite interpolation algorithm. The temperature function along with the derivatives of the winds and temperature with respect to altitude are interpolated at 1/10 km intervals and used to calculate the Richardson number. The probability of occurrence of turbulence is obtained by defining a critical Richardson number ($R_1 = 1$ to $1/4$ according to current literature) and assuming turbulence present when the Richardson number is equal to or less than this value. The probability is then taken as the ratio of the total number of occurrences to the total number of measurements at a 1.0 km level over a season. These seasonal results are then averaged over one km and plotted as in the figure provided. Two techniques are used to establish the seasonal tropopause height. The seasonally averaged temperature gradient value is tested for a sustained change in sign which indicates the change in lapse rate from the troposphere to the stratosphere. Frequently, at high latitudes, the temperature remains fairly constant above the troposphere and through the stratosphere. Since a negative lapse rate may not develop, a second test is used which established the tropopause height as the maximum rate of change in the temperature gradient.

Initial results from stations at low, middle and high latitudes reveal interesting seasonal and latitudinal variation in the occurrence of turbulence as well as particular altitude levels which consistently reveal relatively high occurrences of turbulence. It is also interesting to note that turbulence rapidly decreases at heights which generally agree with those levels reported in models as the tropopause level and follows this pattern as the tropopause level decreases from its highest level in equatorial regions to its lowest levels at high latitudes.

This particular result is substantiated in theory since the stratosphere region above the tropopause level is a dry stable region having a negative temperature lapse rate, and thus the degree of turbulent mixing and transport is greatly reduced from that occurring in the troposphere.

The resolution of the temperature and wind data (100m to a few kilometers) varies with the rise rate of the rawinsonde balloon and the criteria of selecting data points between mandatory levels (those standard milibar height levels recorded at all stations). The fit applied to the data to provide Richardson numbers number determination by possibly introducing effects not present in the thermodynamic structure of the atmosphere. The possibility of obtaining a limited amount of data at suitable sampling intervals to obtain some knowledge of the actual structure in the data has been investigated. Personnel at the Chatham, MA. rawinsonde station have cooperated in the initial investigation by demonstrating the present techniques in data acquisition during a visit to that site in September of 1978. They also provided at that time an analog strip chart recording of temperature along with the standard printout of thermodynamic data. Data points extracted from the temperature analog at the smallest possible interval indicate spectrum wave lengths of approximately a km and longer.

TURBULENCE STUDY - STATISTICAL ANALYSIS

Objectives:

The statistical analysis plan to be described below has two major objectives:

- 1) To relate occurrences of turbulence to latitude, longitude and seasonal variation.
- 2) To identify areas of high turbulence.

I - Site Selection

At present data are available on 144 sites (locations) for the years 1971-1976. From these sites we have selected a subset of 14 sites for initial analysis. This subset has been selected to include:

- 1) A wide range of latitude and longitude. The 14 sets are representative of sites ranging from 70° to 120° longitude (W) and 25° to 50° latitude (N). This will give the results broad applicability.
- 2) "Possibly" interesting variables such as land configurations (i.e. coastal, mountains, flat lands). This will allow us to investigate variables that may introduce variability into our results.
- 3) Stations which are geographically close. This will allow us to investigate the correlation between nearby sites.
- 4) Stations that also have data from 1948 to 1970. This will permit a more extensive time series analysis (if deemed useful).

The results obtained from the 14 selected sites should be representative of locations in the continental United States. When the analysis is completed on these sites data from other sites will be analyzed to act as a validation of the results obtained from the 14 original sites.

II - Data for Analysis

Dependent Variable - The major dependent variable is the proportion of days for a given time period (e.g., a season) with turbulence. Turbulence is determined according to whether the Richardson number is less than .25. At each site we have for a given balloon launch at most one Richardson value for each 1.0k interval from ground level

up to a height of 35 km. A typical situation is to have approximately two balloon launches per day providing two readings for up to 25 km. At this point the balloon usually bursts and measurements are no longer available.

Independent Variable - The independent variables include: site latitude, site longitude, altitude, average temperature, North-South wind speed, East-West wind speed, temperature variation (e.g., range of temperature over a season), density, humidity year, and season (i.e., appropriate time period).

III - Analysis of Individual Sites (First Analysis)

The first analysis is a site-by-site analysis. That is, each site is analyzed individually.

A - Summary Statistics

For a given time period (season) summary statistics on all variables will be computed. These include means, standard deviations, maximums/minimums and ranges for each altitude bins (each 1km is referred to as a bin).

At the present time we are in the stage of the analysis. In particular we are determining the number of altitude bins that can be analyzed with good statistical accuracy and precision. High altitude bins (say above 25 km) often do not have sufficient data for a good analysis. Based on the results we obtain from the 14 selected sites we will determine how many bins should be carried further in our analysis.

B - Altitude Analysis

For each altitude bin, and time period (season) a two-way analysis of variance will be performed using Time Period by year as the variables for classification. The objectives will be: (1) quantify yearly variation and (2) quantify time period variation.

C - Altitude by Time Period by Years Analysis

A three way analysis of variance will be performed. This analysis will quantify variation due to altitude, variation due to years, variation due to time period and interactions among these three sources.

D - Regression Analysis

A multiple regression analysis will be performed. The regression model will relate proportion of turbulence to year, time period, altitude and weather variables such as temperature, density, humidity, wind direction, and interaction of these variables. Specifically, the independent variables are: Year, Time Period, (season or month), Altitude, Average Temperature, Temperature Variation, Wind Direction, (North-South, East-West), Density, Humidity and interaction of these.

IV - Combination of Sites (Second Analysis)

The second analysis consists of combining sites and analyzing them jointly. If deemed necessary the following analysis can be performed on subsets of sites.

A - Regression Analysis (altitude x latitude x longitude)

A regression relating proportion of turbulence to geographic location and altitude will be performed. This regression will also include year and time period (season). The model is

$$\begin{aligned} (\text{Proportion turbulence}) = & b_0 + b_1 (\text{Altitude}) + b_2 (\text{latitude}) + b_3 \\ & (\text{Longitude}) + b_4 (\text{Year}) + b_5 (\text{time period}). \end{aligned}$$

If necessary the model will be expanded to include interactions of the above variables.

B - Expanded Regression Analysis

The next analysis will further expand on the above regressions. Variables which quantify land configurations will be added. Also weather variables as discussed in III D will be added.

V - Logistic Regression

The objective of analysis is to relate occurrence of turbulence to sets of variables. In particular we want to relate variables to the probability of turbulence. A useful model for this is

$$P = \frac{1}{1 + e^{-b_1 X_i + b_0}}$$

where P represents the probability of turbulence and $\sum b_i X_i + b_0$ represents a linear function relating variables X_1, \dots, X_n to the probability P . By use of the transformation

$$\ln \left(\frac{1-P}{P} \right)$$

we have $\ln \left(\frac{1-P}{P} \right) = b_0 + \sum b_i X_i$

and regression analysis is now possible using the transformed dependent variable. We will perform these logistic regressions in addition to the above regressions.

A - Individual Sites

A logistic regression will be performed using variables listed in III D.

B - Combination of Sites

Logistic Regressions will be performed using variables described in IV A and also IV B.

Note: Analysis IV A, IV B, V B will allow us to relate the occurrence of turbulence to latitude, longitude, altitude and seasonal variation. Additionally these analyses will quantify importance of weather variables to turbulence. The functions developed in these analyses, especially the results of V B, will permit us to identify the profiles of variables that relate to higher turbulence - viz, we will be able to identify values of X_1, \dots, X_n given in V that produce high probabilities P given by the logistic regression.

Note: While the above analyses address mainly the problem of explaining past data, we will also investigate their ability to predict turbulence.

Note: As stated earlier the above will first be performed on the 14 selected sites. When this is completed other sites in the continental United States will be analyzed for validation. Then high latitude sites will be selected for ana analysis similar to the one described above.

PROCESSING OF PLASMA FREQUENCY PROBE DATA

1. INTRODUCTION

Purpose of the Experiment

The plasma frequency probe is a rocketborne instrument used for in-situ measurements of electron density and temperature in the E- and F-regions of the ionosphere. This model measures the parallel resonant frequency of an electrically short, RF excited antenna immersed in the ionospheric plasma. Measurements taken can be used to find electron density and temperature and when correlated with altitude, an electron density profile can be derived.

Theory of Operation

The plasma frequency probe (PFP) makes its measurements by finding the parallel resonant frequency of an RF excited antenna.

The RF excitation is generated by mixing the output of a 107 to 147 MHz sweeping oscillator with the outputs of two crystal oscillators (106.5 MHz and 106.4 MHz), resulting in two signals sweeping from 1 to 40 MHz precisely 100 kHz apart. The sweep oscillator is a varactor-tuned oscillator driven by a ramp control voltage, (sweep voltage). This sweep voltage swings from -7.5 to 13 V in 20 ms and then waits at 13 V. As the sweep voltage increases, the frequency at the oscillator output decreases. The two outputs are then filtered and amplified to drive the antenna. The antenna current is measured and this signal is mixed with the second signal from the RF oscillators down to a 100 kHz signal. At parallel resonance, the antenna current is at a minimum causing the output signal from the RF head to be at a minimum. This minimum is then detected by a peak detector.

The peak detector finds a minimum and starts the frequency measuring sequency. At a minimum a flip flop is set, turning on a counter in the sequencer. This counter then counts 1 ms and resets the flip flop in the peak detector making a 1 ms pulse, the timing gate pulse, when a minimum occurs. This timing gate pulse stops the sweep generator, holding the oscillator frequency constant, while also enabling the frequency counter for 1 ms. The output of the counter is the frequency in kHz (in binary) of the minimum. After the sequence is completed, the peak detector is disabled until it is reset by the sequencer at the beginning of the next frame.

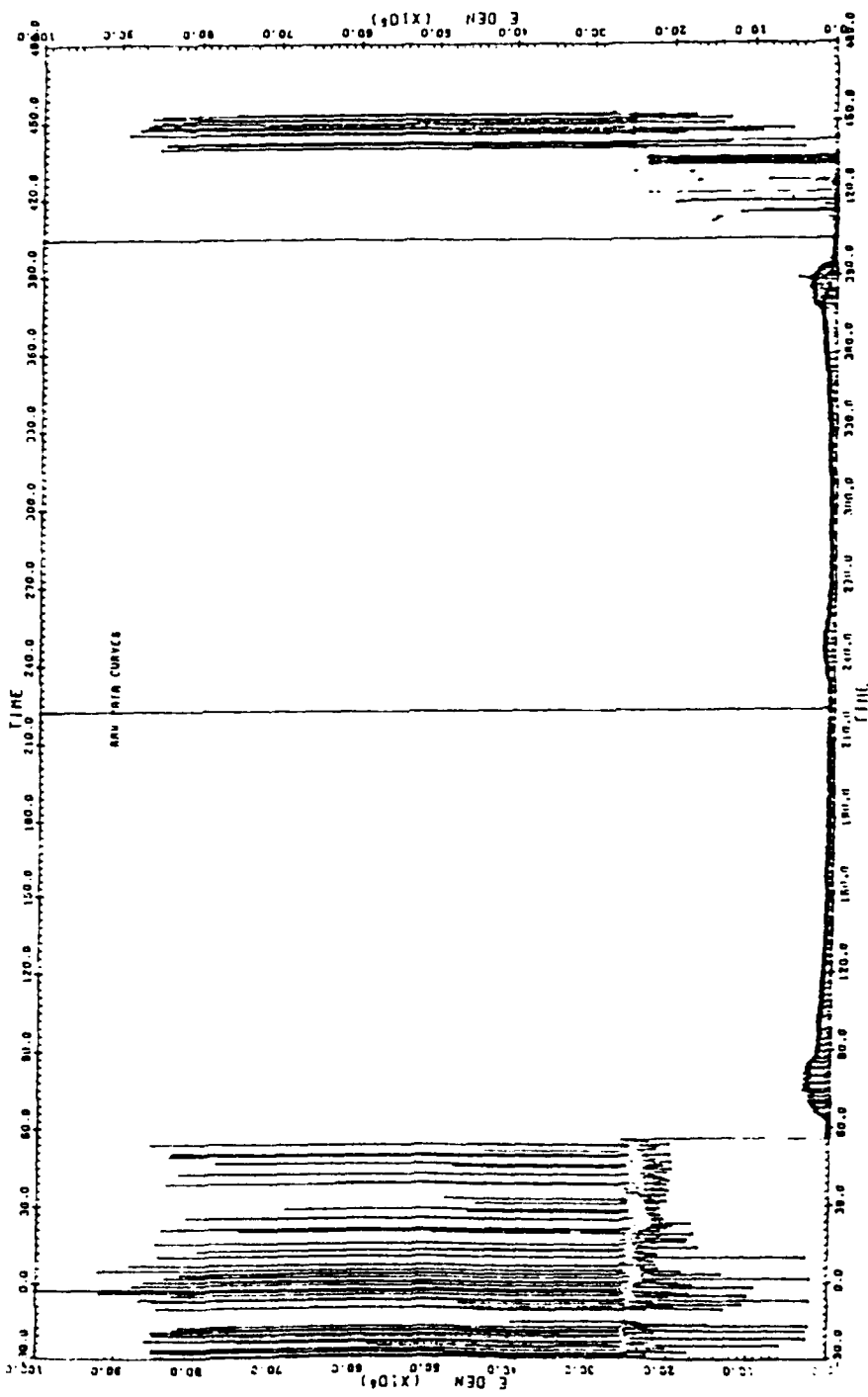
At the end of each frame, the plasma frequency, then stored in counters, is jammed into a shift register. The data is then fed to the buffer amplifier serially during the following frame at a rate of 500 bits per sec. The sequencer generates the reset and jam pulses along with the 500 Hz clock used by the shift register. Also, the sequencer counts the 1 ms pulse.

There are three outputs; the reset pulse, the peak detector output, and the plasma frequency. Each of these is fed through a buffer amplifier to protect the telemetry from over-voltages and at an output impedance of 1k. To give it the correct format, the plasma frequency data is buffered by a variable gain amplifier. The amplifier has a gain of one for the reference bits (the first four bits), and a gain of one-half for the remaining bits.

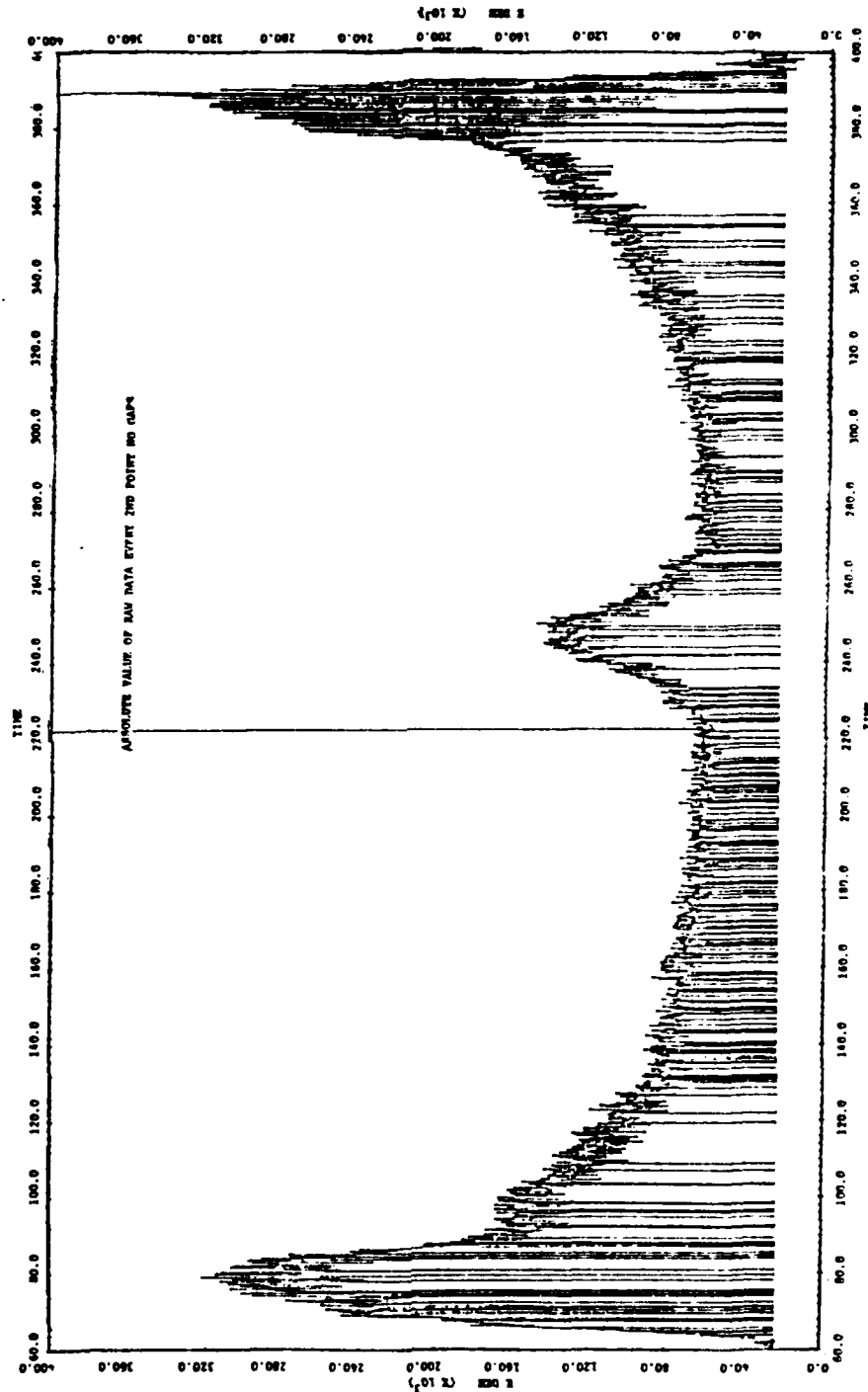
Problems With the Data and Results Obtained

Figures 1 and 2 show the raw electron density data obtained from the experiment. Figure 2 is an expanded view of the interesting portion of the flight upleg and downleg. Due to instrument problems, a very high data drop out rate and system noise level were present.

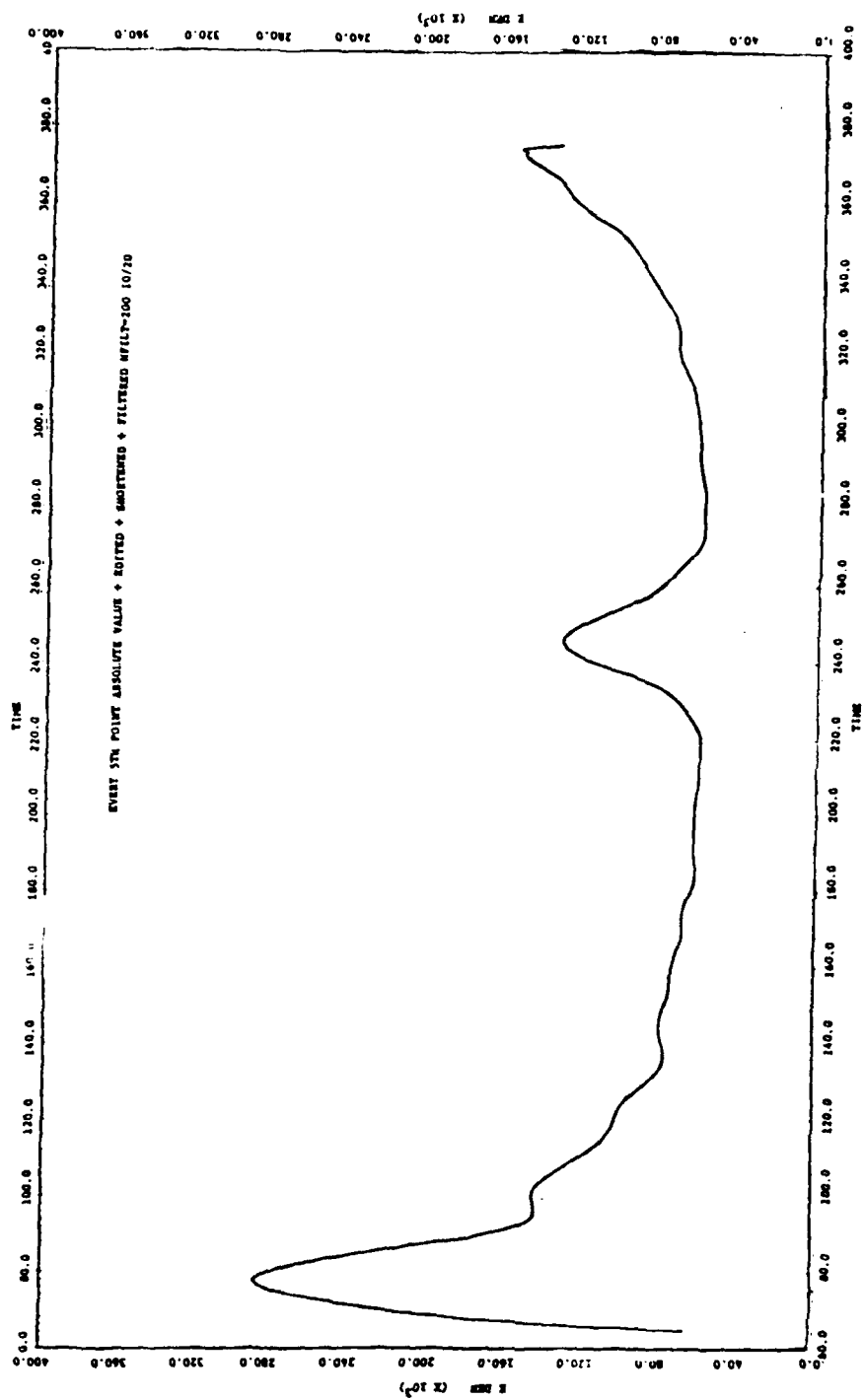
Standard data reduction techniques would be useless with this poor data. However, by applying modern statistical estimation techniques (weighted minimum variance estimation) the electron density profile of Figure 3 was obtained. The weighting was based on the signal bandwidth and the length of the data set available.



RAW ELECTRON DENSITY



EXPANDED VIEW OF UP LEG and DOWN LEG



ELECTRON DENSITY PROFILE ESTIMATE

